Available online at www.sciencedirect.com

SCIENCE DIRECT®

Fluid Dynamics Research 37 (2005) 399–429

FLUID DYNAMICS RESEARCH

Linear and nonlinear sloshing in a circular conical tank[☆]

I.P. Gavrilyuk[a,1], I.A. Lukovsky[b,1], A.N. Timokha[c,*,2]

[a] Berufakademie Thüringen-Staatliche Studienakademie, Am Wartenberg 2, Eisenach, 99817, Germany
[b] Institute of Mathematics, National Academy of Sciences of Ukraine, Tereschenkivska 3, Kiev, 01601, Ukraine
[c] Centre for Ships and Ocean Structures, NTNU, Trondheim, 7491, Norway

Received 8 March 2004; received in revised form 16 April 2005; accepted 10 August 2005

Communicated by M. Oberlack

Abstract

Linear and nonlinear fluid sloshing problems in a circular conical tank are studied in a curvilinear coordinate system. The linear sloshing modes are approximated by a series of the solid spheric harmonics. These modes are used to derive a new nonlinear modal theory based on the Moiseyev asymptotics. The theory makes it possible to both classify steady-state waves occurring due to horizontal resonant excitation and visualise nonlinear wave patterns. Secondary (internal) resonances and shallow fluid sloshing (predicted for the semi-apex angles $\alpha > 60°$) are extensively discussed.

Keywords: Sloshing; Variational method; Nonlinear modal system

1. Introduction

A fluid partly occupying a moving tank undergoes wave motions (sloshing). These motions generate severe hydrodynamic loads that can be dangerous for structural integrity and stability of rockets,

☆ The paper is dedicated to the memory of Maurizio Landrini.
* Corresponding author.
E-mail address: alextim@marin.ntnu.no (A.N. Timokha).
1 Authors are grateful for support made by the German Research Council (DFG).
2 Author acknowledges partial support of the Alexander-von-Humboldt Foundation.

0169-5983/$30.00 © 2005 Published by The Japan Society of Fluid Mechanics and Elsevier B.V.

doi:10.1016/j.fluiddyn.2005.08.004

satellites, ships, trucks and even stationary petroleum containers. If the tank interior is equipped with slosh-suppressing devices, the fluid motions can be accurately modelled by linear theories. Mathematical and numerical aspects of these theories have been documented in NASA Space Vehicle Design Criteria (1968, 1969) and by Abramson (1966), Feschenko et al. (1969) and Rabinovich (1975). Environmental concerns require a new design for tanks of ships, roads and storage systems (Minowa, 1994; Minowa et al., 1994; Faltinsen and Rognebakke, 2000). This suggests double walls, bottom and roof and may as a result increase the total structural weight. A way to avoid the weight penalty consists of removing the slosh-suppressing structures. However, this invalidates linear theories.

Moan and Berge (1997), Cariou and Casella (1999) and Frandsen (2004) reported comparative surveys of the computational fluid dynamics (CFD) methods, which are applicable to nonlinear sloshing problems. By utilising among other programs the commercial FLOW3D-software developed by Flow Science, Inc., Solaas (1995) and Landrini et al. (1999) showed that, if sufficient care is not shown, many of these methods can numerically lose or generate fluid mass and kinetic energy on a long-time scale. An exception is the smoothed particle hydrodynamics (Landrini et al., 2003) method. However, this method is CPU-time inefficient and runs into serious difficulties to identify steady-state fluid wave motions appearing after transients. An alternative to the CFD-methods consists of analytically oriented, modal approaches. Their fundamental aspects have been elaborated by Lukovsky (1990), Faltinsen et al. (2000, 2003), Faltinsen and Timokha (2002b) and La Rocca et al. (1997, 2000). The modal approaches are based on the Fourier representation of the free surface

$$x = f(y, z, t) = \sum \beta_i(t) F_i(y, z) \tag{1}$$

in the $Oxyz$-coordinate system rigidly fixed with a moving tank, where $\{F_i(y, z)\}$ coincides with the linear surface modes. When substituting (1) into the original free boundary problem and using a variational scheme (Lukovsky, 1976, 1990; Miles, 1976; La Rocca et al., 2000; Faltinsen et al., 2000; Shankar and Kidambi, 2002), one can derive an infinite-dimensional system of ordinary differential equations in $\beta_i(t)$ (modal system). Besides, assuming asymptotic relationships between $\beta_i(t)$ truncates this system to a finite-dimensional form. Such an asymptotic truncation may utilise the so-called Moiseyev asymptotics (Narimanov, 1957; Moiseyev, 1958; Ockendon and Ockendon, 1973; Faltinsen, 1974; Dodge et al., 1965; Miles, 1984a,b; Lukovsky, 1990; Solaas and Faltinsen, 1997; Gavrilyuk et al., 2000; Ibrahim et al., 2001; La Rocca et al., 1997; Faltinsen et al., 2000, 2003), for which applicability has been justified in the case of finite fluid depths. Asymptotic relationships of ‘shallow sloshing’ were reported by Chester (1968), Chester and Bones (1968), Ockendon and Ockendon (1973, 2001) and Faltinsen and Timokha (2002a).

An analytical modal basis $\{F_i(y, z)\}$ exists for a very limited set of tank shapes. Among these are tanks of two- or three-dimensional rectangular and vertical circular cylindrical geometry. The modal representation (1) admits the use of approximated $\{F_i(y, z)\}$ (Feschenko et al., 1969; Lukovsky, 1990; Solaas and Faltinsen, 1997), but only if the tank walls are vertical in vicinity of the mean (hydrostatic) free surface. Otherwise, $F_i(y, z),\ i \geqslant 1$, have time-dependent domains of definition. The present paper is devoted to the case of strongly non-vertical (conical) walls. The study is based on a spatial transformation technique proposed by Lukovsky (1975) and developed by Lukovsky and Timokha (2002). This assumes that the original tank cavity can be transformed to an artificial cylindrical domain (in curvilinear coordinates

$(x_1, x_2, x_3))$, where the free surface allows for the normal parametrisation

$$\xi^*(x_1, x_2, x_3, t) = x_1 - f^*(x_2, x_3, t) = 0 \tag{2}$$

and

$$f^*(x_2, x_3, t) = \text{const} + \beta_0(t) + \sum_{i=1}^{\infty} \beta_i(t)\tilde{F}_i(x_2, x_3). \tag{3}$$

After the theoretical preliminaries in Section 2, we define admissible transformations of conical domains. In Section 3, we consider the linear sloshing problem in a curvilinear coordinate system and an analytically oriented variational method for approximating the linear sloshing modes (natural modes). The numerical results are in good agreement with experimental data by Bauer (1982) and Mikishev and Dorozhkin (1961). In Section 4, we derive a nonlinear modal system. This system is based on the Moiseyev asymptotics and generalises analogous modal systems by Dodge et al. (1965), Lukovsky (1990), Gavrilyuk et al. (2000) and Faltinsen et al. (2003) dealing with vertical cylindrical tanks. Shallow fluid flows (quantified for the semi-apex angles $\alpha > 60°$) and secondary resonances (predicted at $\alpha \approx 6°$ and $12°$), which lead to failure of the Moiseyev asymptotics, are not evaluated, but rather discussed. Applicability of the nonlinear modal system is justified in the range $25° < \alpha < 60°$. Analysing periodic solutions of the system, which are associated with resonant steady-state sloshing due to horizontal harmonic excitations with frequencies close to the lowest natural frequency, reveals 'planar' and 'swirling' regimes as well as 'chaotic waves' (both 'planar' and 'swirling' are not stable). Response curves corresponding to 'planar' and 'swirling' are studied. While response curves of the 'planar' regime keep the 'soft-spring' behaviour for $\alpha < 60°$, 'swirling' demonstrates transition from the 'hard-spring' to 'soft-spring' behaviour as α passes through $\approx 41.1°$ (to the authors knowledge, this critical angle has never been estimated in the scientific literature). These and other results on steady-state resonant motions are compared with analogous results established for sloshing in a circular cylindrical tank (Abramson, 1966; Miles, 1984a,b; Lukovsky, 1990; Gavrilyuk et al., 2000).

2. Theoretical preliminaries

2.1. Free boundary problem

We consider wave motions of an incompressible perfect fluid partly occupying a rigid mobile tank Q (Fig. 1). The motions are described in a non-inertial Cartesian system $Oxyz$ rigidly fixed with the tank. Motions of the tank are described in an absolute Cartesian coordinate system $O'x'y'z'$ by the pair of time-dependent vectors $\boldsymbol{v}_O(t)$ and $\boldsymbol{\omega}(t)$. These vectors denote translatory and angular velocities of the $Oxyz$-frame, respectively. Since any absolute position vector $\boldsymbol{r}'(t) = (x', y', z')$ can be decomposed into the sum of $\boldsymbol{r}'_O(t) = \vec{O'O}$ and the relative position vector $\boldsymbol{r} = (x, y, z)$, the gravity potential U depends on (t, x, y, z), i.e. $U(x, y, z, t) = -\boldsymbol{g}\cdot\boldsymbol{r}'$, $\boldsymbol{r}' = \boldsymbol{r}'_O + \boldsymbol{r}$, where $\boldsymbol{g}$ is the gravity acceleration vector. Furthermore, we assume irrotational potential fluid flows and introduce the velocity potential $\Phi(x, y, z, t)$. The following free boundary problem (derived for instance by Narimanov et al., 1977; Lukovsky, 1990, 2004) couples

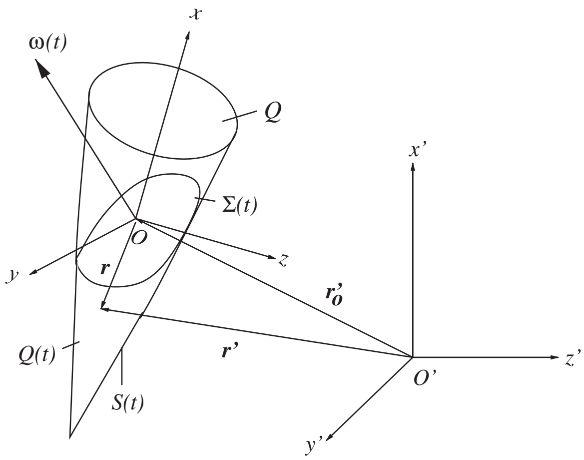

Fig. 1. Sketch of a moving conical tank.

$\Phi(x, y, z, t)$ and the fluid shape $Q(t)$ (defined by the equation $\xi(x, y, z, t) = 0$)

$$\Delta\Phi = 0 \quad \text{in } Q(t), \tag{4a}$$

$$\frac{\partial \Phi}{\partial \nu} = \boldsymbol{v}_0 \cdot \boldsymbol{\nu} + \boldsymbol{\omega} \cdot [\boldsymbol{r} \times \boldsymbol{\nu}] \quad \text{on } S(t), \tag{4b}$$

$$\frac{\partial \Phi}{\partial \nu} = \boldsymbol{v}_0 \cdot \boldsymbol{\nu} + \boldsymbol{\omega} \cdot [\boldsymbol{r} \times \boldsymbol{\nu}] - \frac{\partial \xi}{\partial t} / |\nabla \xi| \quad \text{on } \Sigma(t), \tag{4c}$$

$$\frac{\partial \Phi}{\partial t} + \frac{1}{2}(\nabla\Phi)^2 - \nabla\Phi \cdot (\boldsymbol{v}_0 + \boldsymbol{\omega} \times \boldsymbol{r}) + U = 0 \quad \text{on } \Sigma(t), \tag{4d}$$

$$\int_{Q(t)} \mathrm{d}Q = \text{const}, \tag{4e}$$

where $S(t)$ is the wetted walls and bottom, $\Sigma(t)$ is the free surface and $\boldsymbol{\nu}$ is the outer normal.

The evolutional free boundary problem (4) should be completed by initial conditions. They define the initial fluid shape and velocity as follows:

$$\xi(x, y, z, t_0) = \xi_0(x, y, z); \quad \frac{\partial \xi}{\partial t}(x, y, z, t_0) = \xi_1(x, y, z), \tag{5}$$

where ξ_0 and ξ_1 are known.

2.2. Transformations

Let us consider an open artificial cylindrical domain $Q^* = (0, d) \times D$ in the $Ox_1x_2x_3$-coordinate system and let Q be the interior of a rigid tank in the $Oxyz$-system. We define smooth transformations that map Q to Q^* and back as follows:

$$\begin{aligned} &x_1 = x, \quad x_2 = x_2(x, y, z), \quad x_3 = x_3(x, y, z); \\ &x = x_1, \quad y = y(x_1, x_2, x_3), \quad z = z(x_1, x_2, x_3). \end{aligned} \tag{6}$$

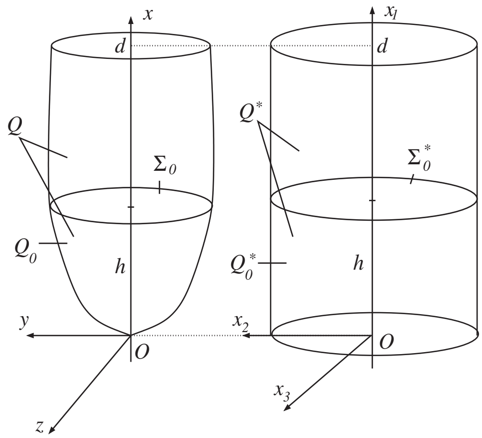

Fig. 2. Sketch of an admissible transformation.

Here, the Oyz-plane has to be tangent to $S = \partial Q$ and $x > 0$ for $(x, y, z) \in Q$ and the Ox_2x_3-plane should be superposed with the bottom of Q^* (Fig. 2). Transformations (6) are also obligated to have the positive Jacobian

$$J^*(x_1, x_2, x_3) = \frac{D(x, y, z)}{D(x_1, x_2, x_3)}, \quad (J(x, y, z) = 1/J^*) \tag{7}$$

inside of Q^* and, except a limited set of isolated points, on the boundary $S^* = \partial Q^*$. Such a single point with $J^* = 0$ invertible appears for conical, parabolic, etc. domains, because (6) maps the bottom of Q^* to the origin O (the situation is schematically depicted in Fig. 2).

2.2.1. Linear natural modes

If $\boldsymbol{v} = \boldsymbol{\omega} = \mathbf{0}$, the free boundary problem (4) can be linearised relative to the trivial solution $\xi = z +$ const, $\Phi =$ const, which determines a hydrostatic fluid shape Q_0 (Fig. 2). The linearisation implies the smallness of $\nabla\Phi$ and ∇f $(\Sigma(t) : x = f(t, y, z))$, and, apparently, becomes mathematically justified only in a curvilinear coordinate system. The procedure includes transformation (6) (admitting (2)–(3)), evaluates (4) in the (x_1x_2, x_3)-coordinates, assumes $|\Phi^*| \sim |f^* - h| \sim |\nabla^*\Phi| \sim |\nabla^* f^*| = O(\varepsilon) \ll 1$ and, finally, neglects the $o(\varepsilon)$-term. After linearising (4), we set up $\Phi^* = \mathrm{i}\sqrt{g\kappa}\phi^*(x_1, x_2, x_3)\exp(\mathrm{i}\sqrt{g\kappa}t)$; $f^* = \exp(\mathrm{i}\sqrt{g\kappa}t)F(x_1, x_2)$ and obtain a spectral boundary problem in $Q_0^* = (0, h) \times D$. In accordance with theorems proved by Lukovsky and Timokha (2002), this spectral problem is isomorphically equivalent to

$$\Delta\phi = 0 \quad \text{in } Q_0; \qquad \frac{\partial\phi}{\partial v} = 0 \quad \text{on } S_0; \qquad \frac{\partial\phi}{\partial z} = \kappa\phi \quad \text{on } \Sigma_0; \qquad \int_{\Sigma_0} \frac{\partial\phi}{\partial z}\,\mathrm{d}y\,\mathrm{d}z = 0, \tag{8}$$

which is considered in the (x, y, z)-coordinates (Feschenko et al., 1969).

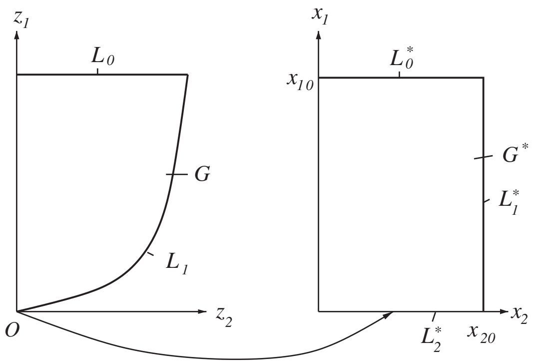

Fig. 3. Transformations of the meridional cross-section.

If Q_0 is of an axial-symmetric shape, admissible transformations of Q_0 to Q_0^* can be combined with separation of spatial variables. This leads to an infinite series of two-dimensional spectral problems in a rectangular domain. Reduction to these two-dimensional problems includes two steps. The first step implies the substitution

$$x = z_1, \quad y = z_2 \cos z_3, \quad z = z_2 \sin z_3 \tag{9}$$

together with expression for ϕ:

$$\phi_m(z_1, z_2, z_3) = \psi_m(z_1, z_2)^{\cos}_{\sin}(mz_3), \quad m = 0, 1, 2, \ldots \, . \tag{10}$$

Inserting (9)–(10) into (8) leads to the following family of spectral problems in the meridional plane Oz_2z_1:

$$\begin{gathered}\frac{\partial}{\partial z_2}\left(z_2 \frac{\partial \psi_m}{\partial z_1}\right) + \frac{\partial}{\partial z_2}\left(z_2 \frac{\partial \psi_m}{\partial z_2}\right) - \frac{m^2}{z_2}\psi_m = 0 \quad \text{in } G; \qquad \frac{\partial \psi_m}{\partial z_2} = \kappa \psi_m \quad \text{on } L_0, \\ \frac{\partial \psi_m}{\partial \nu} = 0 \quad \text{on } L_1; \qquad |\psi_m(z_1, 0)| < \infty, \quad m = 0, 1, 2, \ldots, \int_{L_0} \psi_0 z_2 \, \mathrm{d}z_2 = 0,\end{gathered} \tag{11}$$

where L_0 and L_1 are the boundaries of G (see Fig. 3); $\boldsymbol{\nu}$ is the outer normal to L_1 (theory of (11) is given by Lukovsky et al., 1984).

The second step assumes

$$z_1 = x_1, \quad z_2 = \zeta(x_1, x_2), \quad (z_3 = x_3), \tag{12}$$

which maps G to G^* as shown in Fig. 3 ($L_0 \to L_0^*, L_1 \to L_1^*$). In the $Ox_1x_2x_3$-coordinate system, the spectral problems (11) take the form

$$\begin{aligned} &p \frac{\partial^2 \psi_m}{\partial x_1^2} + 2q \frac{\partial^2 \psi_m}{\partial x_1 \partial x_2} + s \frac{\partial^2 \psi_m}{\partial x_2^2} + \left(\frac{\partial p}{\partial x_1} + \frac{\partial q}{\partial x_2}\right)\frac{\partial \psi_m}{\partial x_1} \\ &\quad + \left(\frac{\partial s}{\partial x_2} + \frac{\partial q}{\partial x_1}\right)\frac{\partial \psi_m}{\partial x_2} - cm^2 \psi_m = 0 \quad \text{in } G^*, \end{aligned}$$

$$p\,\frac{\partial\psi_m}{\partial x_1}+q\,\frac{\partial\psi_m}{\partial x_2}=\kappa p\psi_m \quad \text{on } L_0^*; \qquad s\,\frac{\partial\psi_m}{\partial x_2}+q\,\frac{\partial\psi_m}{\partial x_1}=0 \quad \text{on } L_1^*,$$
$$\int_0^{x_{20}}\psi_0\zeta\,\frac{\partial\zeta}{\partial x_2}\,\mathrm{d}x_2=0, \quad m=0,1,2,\ldots, \tag{13}$$

where

$$p(x_1,x_2)=\zeta\,\frac{\partial\zeta}{\partial x_2}; \quad q(x_1,x_2)=pa; \quad s(x_1,x_2)=p(a^2+b^2),$$
$$a(x_1,x_2)=\frac{\partial x_2}{\partial\zeta}; \quad b(x_1,x_2)=\frac{\partial x_1}{\partial\zeta}; \quad c(x_1,x_2)=\frac{1}{\zeta}\,\frac{\partial\zeta}{\partial x_2}. \tag{14}$$

As shown by Lukovsky and Timokha (2002), problem (13) does not need any boundary conditions on the artificial bottom L_2^* and along $x_2=0$. However, ψ_m should be bounded at $x_1=0$ and $x_2=0$, simultaneously.

2.2.2. Nonlinear modal system

We employ the Bateman–Luke variational formulation of (4):

$$\delta W(\Phi,\xi)=\delta\int_{t_1}^{t_2}L\,\mathrm{d}t=0;$$
$$L=\int_{Q(t)}(p-p_0)\,\mathrm{d}Q=-\rho\int_{Q(t)}\left[\frac{\partial\Phi}{\partial t}+\frac{1}{2}(\nabla\Phi)^2-\nabla\Phi\cdot(\boldsymbol{v}_0+\boldsymbol{\omega}\times\boldsymbol{r})+U\right]\mathrm{d}Q, \tag{15a}$$
$$\delta\Phi|_{t_1,t_2}=0; \quad \delta\xi|_{t_1,t_2}=0. \tag{15b}$$

Here, the nonlinear functional (15a) is based on the pressure-integral Lagrangian. Lukovsky and Timokha (2002) have mathematically established that the Lagrangian (15a) is invariant relative to transformations (6), namely,

$$L\equiv L^*=-\rho\int_{Q^*(t)}\left[\frac{\partial\Phi^*}{\partial t}+\frac{1}{2}(\nabla^*\Phi^*)^2-\nabla^*\Phi^*\cdot(\boldsymbol{v}_0+\boldsymbol{\omega}\times\boldsymbol{r})^*+U^*\right]J^*\,\mathrm{d}Q^*, \tag{16}$$

where $Q^*(t)$ is the transformed domain,

$$U^*=U(x(x_1,x_2,x_3),\,y(x_1,x_2,x_3),\,z(x_1,x_2,x_3),\,t),$$
$$\Phi^*=\Phi(x(x_1,x_2,x_3),\,y(x_1,x_2,x_3),\,z(x_1,x_2,x_3),\,t),$$
$$\nabla\Phi=\nabla^*\Phi^*=\left(g^{1,j}\,\frac{\partial\Phi^*}{\partial x_j},\,g^{2,j}\,\frac{\partial\Phi^*}{\partial x_j},\,g^{3,j}\,\frac{\partial\Phi^*}{\partial x_j}\right),$$

and

$$g^{i,j}=\frac{\partial\boldsymbol{r}}{\partial x_i}\,\frac{\partial\boldsymbol{r}}{\partial x_j}, \quad i,j=1,2,3,$$

is the metric tensor (stars in $(\boldsymbol{v}_0+\boldsymbol{\omega}\times\boldsymbol{r})^*$ denote projections on the unit vectors of a curvilinear coordinate system).

By adopting derivations (based on (15)) of nonlinear modal systems by Lukovsky (1990) and Faltinsen et al. (2000) and the modal solutions

$$f^* = x_{10} + \beta_0(t) + \sum_{i=1}^{\infty} \beta_i(t) \tilde{F}_i(x_2, x_3), \tag{17a}$$

$$\Phi^* = \boldsymbol{v}_0 \cdot \boldsymbol{r} + \sum_{n=1}^{\infty} Z_n(t) \phi_n(x_1, x_2, x_3), \tag{17b}$$

where $x_{10} = h$, $\{\tilde{F}_i(x_2, x_3)\}$, $\{\phi_n(x_1, x_2, x_3)\}$ are the basic systems of functions on Σ_0^* and in Q_0^*, respectively, and, for brevity, $\boldsymbol{\omega} = \mathbf{0}$, we get the following infinite-dimensional nonlinear modal system:

$$\frac{\mathrm{d}}{\mathrm{d}t} A_n - \sum_k A_{nk} Z_k = 0, \quad n = 1, 2, \ldots, \tag{18a}$$

$$\sum_n \dot{Z}_n \frac{\partial A_n}{\partial \beta_i} + \frac{1}{2} \sum_{nk} \frac{\partial A_{nk}}{\partial \beta_i} Z_n Z_k + (\dot{v}_{01} - g_1) \frac{\partial l_1}{\partial \beta_i}$$
$$+ (\dot{v}_{02} - g_2) \frac{\partial l_2}{\partial \beta_i} + (\dot{v}_{03} - g_3) \frac{\partial l_3}{\partial \beta_i} = 0, \quad i = 1, 2, \ldots . \tag{18b}$$

This system couples the generalised coordinates $Z_n(t)$, $\beta_i(t)$ and $A_n(\beta_i)$, $A_{nk}(\beta_i)$, $l_k(\beta_i)$ defined by the integrals

$$A_n = \rho \int_D \left(\int_0^{f^*} \phi_n J^* \, \mathrm{d}x_1 \right) \mathrm{d}x_2 \, \mathrm{d}x_3; \quad A_{nk} = \rho \int_D \left(\int_0^{f^*} (\nabla^* \phi_n^*, \nabla^* \phi_k^*) J^* \, \mathrm{d}x_1 \right) \mathrm{d}x_2 \, \mathrm{d}x_3, \tag{19}$$

$$\frac{\partial l_1}{\partial \beta_i} = \rho \int_{\Sigma_0^*} F_i [x_1 J^*(x_1, x_2, x_3)]_{x_1 = f^*} \, \mathrm{d}x_2 \, \mathrm{d}x_3,$$
$$\frac{\partial l_2}{\partial \beta_i} = \rho \int_{\Sigma_0^*} F_i [y(x_1, x_2, x_3) J^*(x_1, x_2, x_3)]_{x_1 = f^*} \, \mathrm{d}x_2 \, \mathrm{d}x_3,$$
$$\frac{\partial l_3}{\partial \beta_i} = \rho \int_{\Sigma_0^*} F_i [z(x_1, x_2, x_3) J^*(x_1, x_2, x_3)]_{x_1 = f^*} \, \mathrm{d}x_2 \, \mathrm{d}x_3 \tag{20}$$

(the upper limit f^* in integrals (19) depends on $\beta_i(t)$ due to (17a)).

3. Linear sloshing in a circular conical tank

Numerical solutions of the spectral problem (8) in a conical domain Q_0 can be found by diverse methods based on spatial discretisation (Solaas, 1995; Solaas and Faltinsen, 1997). However, because these discrete solutions $\{\phi_n\}$ are not expandable over the mean free surface Σ_0, their usage in (19) is generally impossible. To the authors' knowledge, the current scientific literature contains only two numerical approaches to (8) which give satisfactory approximations of eigenfunctions $\{\phi_n\}$ to be used as a basis in the variational scheme of Section 2.2.2. The first approach is based on the Treftz method with the harmonic polynomials as a functional basis. Results by Feschenko et al. (1969) showed applicability

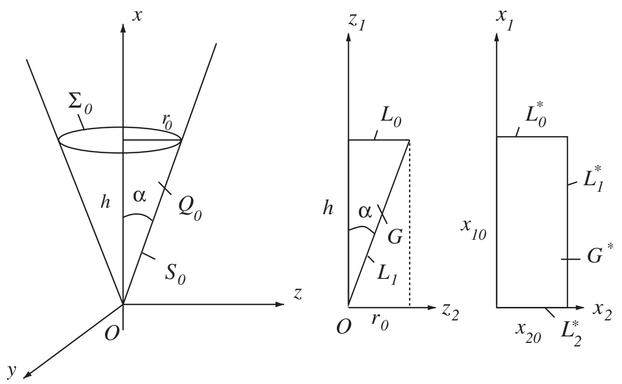

Fig. 4. Sketch of a conical tank, its meridional cross-section G and the transformed domain G^*; $x_{10} = h$, $x_{20} = \tan\alpha$.

of this approach for computing both eigenvalues and eigenfunctions. The approximate eigenfunctions are harmonic in space and, therefore, expandable over Σ_0. However, because the approximate $\{\phi_n\}$ does not satisfy zero-Neumann condition on conical walls over Σ_0, inserting them into (19) can lead to a numerical error for certain evolutions of $Q(t)$. Physically, the error may be treated as inlet/outlet through the rigid walls over Σ_0.

Another appropriate analytically oriented approach to (8) in a conical domain was reported by Dokuchaev (1964), Bauer (1982), Lukovsky and Bilyk (1985) and Bauer and Eidel (1988). It consists of replacing the planar surface Σ_0 by an artificial spheric segment. In that case, problem (8) has analytical solutions which coincide with the solid spheric harmonics. Bauer (1982) has shown that an error caused by the replacement is small for relatively small α, his numerical examples agreed well with model tests for $\alpha < \pi/12(\text{rad}) = 15^\circ$.

Combining these two approaches, we will adopt the solid spheric harmonics appearing in the papers by Bauer (1982) and Dokuchaev (1964) as a functional basis in the variational method by Feschenko et al. (1969) (instead of the harmonic polynomials). The method will be elaborated in the (x_1, x_2, x_3)-coordinates, so that the linear natural modes (eigenfunctions) can be substituted into (17), (19) and (20).

3.1. Natural modes

In accordance with definitions in Fig. 4, we superpose the origin O with the apex of an inverted cone and direct the Ox-axis upwards. In that case, the cone is determined by the equation $x = \cot\alpha\sqrt{y^2 + z^2}$ and the mean free surface $\Sigma_0(x = h)$ is a circle of radius $r_0 = h\tan\alpha$, where h is the fluid depth. By substituting $x := x/r_0, y := y/r_0, z := z/r_0$, we get a non-dimensional formulation of the spectral problem (8). Finally, the resulting transformation (9) + (12) is proposed,

$$x = x_1; \quad y = x_1 x_2 \cos x_3; \quad z = x_1 x_2 \sin x_3, \tag{21a}$$

$$x_1 = \frac{x}{r_0}; \quad x_2 = \sqrt{\frac{y^2 + z^2}{x^2}}; \quad x_3 = \arctan\frac{z}{y}, \tag{21b}$$

so that (13) takes the following form:

$$x_1^2 x_2 \frac{\partial^2 \psi_m}{\partial x_1^2} - 2x_1 x_2^2 \frac{\partial^2 \psi_m}{\partial x_1 \partial x_2} + x_2(1+x_2^2)\frac{\partial^2 \psi_m}{\partial x_2^2} + (1+2x_2^2)\frac{\partial \psi_m}{\partial x_2} - \frac{m^2}{x_2}\psi_m = 0 \quad \text{in } G^*, \tag{22a}$$

$$x_1^2 x_2 \frac{\partial \psi_m}{\partial x_1} - x_1 x_2^2 \frac{\partial \psi_m}{\partial x_2} = \kappa_m x_1^2 x_2 \psi_m \quad \text{on } L_0^*, \tag{22b}$$

$$x_2(x_2^2+1)\frac{\partial \psi_m}{\partial x_2} - x_1 x_2^2 \frac{\partial \psi_m}{\partial x_1} = 0 \quad \text{on } L_1^*, \quad m = 0, 1, 2, \ldots, \tag{22c}$$

$$\int_0^{x_{20}} \psi_0 x_2 \, dx_2 = 0 \quad \text{as } m = 0, \tag{22d}$$

where $G^* = \{(x_1, x_2) : 0 \leqslant x_1 \leqslant x_{01}, 0 \leqslant x_2 \leqslant x_{20}\}$, $x_{20} = \tan\alpha$, $x_{10} = h/r_0 = 1/x_{20}$ and

$$a = -\frac{x_2}{x_1}; \quad b = \frac{1}{x_1}; \quad p = x_1^2 x_2; \quad q = -x_1 x_2^2; \quad s = x_2(x_2^2+1); \quad c = \frac{1}{x_2}.$$

Each nth eigenvalue of (22), κ_{mn}, computes the natural circular frequency

$$\sigma_{mn} = \sqrt{\frac{g\kappa_{mn}}{r_0}} = \sqrt{\frac{g\kappa_{mn}}{h\tan\alpha}}. \tag{23}$$

The surface sloshing modes are defined by ψ_m as follows:

$$x_1 = F_{mn}(x_2, x_3) = \phi_{mn}(x_{10}, x_2, x_3); \quad 0 \leqslant x_2 \leqslant x_{20}, \quad 0 \leqslant x_3 \leqslant 2\pi, \tag{24}$$

where

$$\phi_{mn}(x_1, x_2, x_3) = \psi_{mn}(x_1, x_2)^{\cos}_{\sin} m x_3 \tag{25}$$

is the nth eigenfunction of (22) corresponding to κ_{mn}.

3.2. Approximate natural modes

3.2.1. Separation of spatial variables

As proved by Eisenhart (1934), the Laplace equation allows for separation of spatial variables only in 17 inequivalent coordinate systems. The $Ox_1x_2x_3$-coordinate system defined by (21a) belongs to the admissible set. The separability of (22a) and (22c) leads to the following particular solutions $\psi_m[v](x_1, x_2) = w_v^{(m)}(x_1, x_2) = (x_1/x_{10})^v v_v^{(m)}(x_2)$, where

$$x_2(1+x_2^2) v_v^{(m)''} + (1 + 2x_2^2 - 2vx_2^2) v_v^{(m)'} + \left[v(v-1)x_2 - \frac{m^2}{x_2}\right] v_v^{(m)} = 0, \quad |v_v^{(m)}(0)| < \infty, \tag{26a}$$

$$v_v^{(m)'}(x_{20}) = v \frac{x_{20}}{1+x_{20}^2} v_v^{(m)}(x_{20}), \quad m = 0, 1, \ldots, v \geqslant m. \tag{26b}$$

Eqs. (26a), (26b) constitute the v-parametric boundary value problem, which has non-trivial solutions only for certain values of v. If we input a test v in the differential (26a) and output $v_v^{(m)\prime}(x_{20})$ and $v_v^{(m)}(x_{20})$, the boundary condition (26b) plays the role of a transcendental equation with respect to v. This transcendental equation can be solved by means of an iterative algorithm.

In order to get an approximate $\psi_{mn}(x_1, x_2)$, we should fix m and calculate q lower roots $\{v_{m1} < v_{m2} < \cdots < v_{mq}\}$ of this transcendental equation. The nth ($1 \leqslant n \leqslant q$) approximate solution of (22), which corresponds to κ_{mn}, can then be posed as

$$\psi_{mn}(x_1, x_2) = \sum_{k=0}^{q} \bar{a}_{nk}^{(m)} \left(\frac{x_1}{x_{10}}\right)^{v_{mk}} v_{v_{mk}}^{(m)}(x_2), \tag{27}$$

where coefficients $\bar{a}_{nk}^{(m)}$ have to satisfy the supplementary conditions

$$\bar{a}_{n0}^{(m)} = \begin{cases} 0, & m \neq 0, \\ -\sum_{k=1}^{q} \bar{a}_{nk}^{(m)} c_{v_{0k}}, & m = 0, \end{cases} \qquad c_{v_{0k}} = \frac{2}{x_{20}^2} \int_0^{x_{20}} w_{v_{0k}}^{(0)}(x_{10}, x_2) x_2 \, \mathrm{d}x_2$$

($v_{m0} = 0$, $v_{v_{m0}}^{(m)} = 1$) to agree with (22d).

One should note that comparing $v_v^{(0)}$ with the Legendre function P_v^0 deduces

$$v_v^{(0)}(x_2) = \left(\sqrt{1 + x_2^2}\right)^v P_v^0 \left(1/\sqrt{1 + x_2^2}\right). \tag{28}$$

In view of this point,

$$P_v^0 \left(1 \Big/ \sqrt{1 + x_2^2}\right) = \sum_{p=1}^{\infty} \frac{(v - p + 1)(v - p + 1) \cdots (v + p)}{(p!)^2} \left(\frac{1}{2\sqrt{1 + x_2^2}} - \frac{1}{2}\right)^p \tag{29}$$

(Bateman and Erdelyi, 1953) and recurrence formulae for P_v^m (Lukovsky et al., 1984) re-written to the (x_2, x_3)-coordinates

$$\begin{aligned} &(v + m + 1) v_{v+1}^{(m)} = (2v + 1) v_v^{(m)} - (v - m)(1 + x_2^2) v_{v-1}^{(m)}, \\ &(v + m + 1) x_2 v_v^{(m+1)} = 2(m + 1)[(1 + x_2^2) v_{v-1}^{(m)} - v_v^{(m)}], \\ &\frac{\mathrm{d} v_v^{(m)}}{\mathrm{d} x_2} = \frac{1}{x_2} [v v_v^{(m)} - (v - m) v_{v-1}^{(m)}] \end{aligned} \tag{30}$$

facilitate computing $v_v^{(m)\prime}(x_2)$ and $v_v^{(m)}(x_2)$ for arbitrary x_2, m and $v \geqslant m$.

3.2.2. *The Treftz method based on* (27)

Representation (27) and the Rayleigh–Kelvin minimax principle for the spectral problems (22) (see, Feschenko et al., 1969) make it possible to compute approximate eigenvalues κ_{mn}. The numerical scheme implies

$$\frac{\partial J_m}{\partial \bar{a}_{ni}^{(m)}} = 0, \quad i = 1, 2, \ldots, q; \quad m = 0, 1, 2, \ldots, \tag{31a}$$

$$J_m = \int_{G^*}\left[p\left(\frac{\partial\psi_m}{\partial x_1}\right)^2 + 2q\,\frac{\partial\psi_m}{\partial x_1}\,\frac{\partial\psi_m}{\partial x_2} + s\left(\frac{\partial\psi_m}{\partial x_2}\right)^2 + \frac{m^2}{x_2}\,\psi_m^2\right]\mathrm{d}x_1\,\mathrm{d}x_2 - \kappa\int_{L_0^*} p\psi_m^2\,\mathrm{d}x_2, \quad m = 0, 1, \ldots, \tag{31b}$$

and, as a consequence, leads to the spectral matrix problem

$$\det|\{\alpha_{ij}^{(m)}\} - \kappa\{b_{ij}^{(m)}\}| = 0, \quad i, j = 1, \ldots, q, \tag{32}$$

where the symmetric positive matrices $\{\alpha_{ij}^{(m)}\}$ and $\{b_{ij}^{(m)}\}$ are calculated by the following formulae:

$$b_{ij}^{(m)} = x_{10}^2\int_0^{x_{20}} x_2 w_{v_{mi}}^{(m)} w_{v_{mj}}^{(m)}\,\mathrm{d}x_2, \quad i, j = 1, \ldots, q, \tag{33}$$

$$\alpha_{ij}^{(m)} = x_{10}\int_0^{x_{20}} x_2\left\{\left[x_{10}\frac{\partial w_{v_{mi}}^{(m)}}{\partial x_1} - x_2\frac{\partial w_{v_{mi}}}{\partial x_2}\right] w_{v_{mj}}^{(m)}\right\}_{x_1 = x_{10}}\mathrm{d}x_2, \quad i, j = 1, \ldots, q. \tag{34}$$

The spectral problem (32) gives not only approximate eigenvalues, but also eigenvectors expressed in terms of coefficients $\{\bar{a}_{nk}^{(m)},\ k = 1, \ldots, q\},\ n = 1, \ldots, q$. Being substituted into (27), these eigenvectors determine eigenfunctions $\psi_{mn}(x_1, x_2),\ n = 1, \ldots, q$.

3.2.3. Convergence

Furthermore, positive eigenvalues $\{\kappa_{mn},\ n = 1, \ldots, q\}$ of (32) are posed in ascending order. Fixing m and evaluating some of the lower approximate κ_{mn} versus q (see Table 1), one displays convergence of the Treftz method. Our numerical experiments with $\kappa_{m1},\ m \geqslant 0$, showed that 5–6 basis functions ($q = 5$ or 6) guarantee 5–6 significant figures, in general, and 10–12 significant figures for $\alpha \geqslant 45°$, in particular. Weaker convergence for smaller α can be treated in terms of the mean fluid depth $x_{10} = h$ and geometric proportions of Q_0 versus α. If $\alpha \to 0$ then $x_{10} \to \infty$ and Q_0 becomes geometrically similar to a fairly long circular cylinder. The linear sloshing modes (eigenfunctions of (8)) in a circular cylindrical tank are characterised by exponential decaying from Σ_0 to the bottom (Abramson, 1966; Lukovsky et al., 1984; Gavrilyuk et al., 2000), but, in contrast, functions (27) have power asymptotics.

3.2.4. Natural frequencies versus α

Fig. 5 shows that κ_{mn} and, therefore, σ_{mn}, which are defined by (23), decrease monotonically with increasing α. Besides, a general tendency consists of $\kappa_{mn} \to 0$ as $\alpha \to 90°$, but each eigenvalue κ_{mn} has a proper decaying gradient. As a result, some of the natural frequencies may become equal at an isolated α. We demonstrate this fact by points A and B in Fig. 5. The point A corresponds to $\alpha \approx 19.2°$, where $\sigma_{31} = \sigma_{01}$, and B occurs at $\alpha \approx 30°$, where $\sigma_{12} = \sigma_{51}$.

In accordance with theorems by Feschenko et al. (1969), problem (8) has a denumerable set of real positive eigenvalues and each κ_{mn} continuously depends on smooth deformations of Q_0. Both appearance and 'split' of multiple eigenvalues are consistent with these theorems. Moreover, the matrices $\{\alpha_{ij}^{(m)}\}$ and $\{b_{ij}^{(m)}\}$ are symmetric and positive and, therefore, the crossings in Fig. 5 do not yield a numerical difficulty in solving (32) (Parlett, 1998). On the other hand, Bauer et al. (1975) and Bridges (1987) showed that

Table 1
κ_{mn} versus q in (27)

$\alpha=\pi/20$(rad) $=9^\circ$, $x_{10}=6.31375151$							
q	κ_{11}	κ_{21}	κ_{01}	κ_{31}	κ_{41}	κ_{12}	κ_{51}
2	1.691615430	2.845734973	3.740941260	3.940773781	5.009527439	5.250674149	6.063005004
3	1.691607322	2.845702193	3.740763366	3.940706201	5.009419535	5.240481474	6.062853900
4	1.691606215	2.845697065	3.740735620	3.940694662	5.009399941	5.240034153	6.062825178
5	1.691605959	2.845695769	3.740728597	3.940691547	5.009394389	5.239957174	6.062816727
6	1.691605890	2.845695338	3.740726259	3.940690460	5.009392374	5.239936238	6.062813563
$\alpha=\pi/18$(rad) $=10^\circ$, $x_{10}=5.67128182$							
q	κ_{11}	κ_{21}	κ_{01}	κ_{31}	κ_{41}	κ_{12}	κ_{51}
2	1.674354687	2.821056165	3.729116268	3.909489499	4.972117607	5.241575140	6.019801612
3	1.674345993	2.821020466	3.728919662	3.909415640	4.971999653	5.229299109	6.019636623
4	1.674344847	2.821015056	3.728889858	3.909403387	4.971978802	5.228803377	6.019606045
5	1.674344590	2.821013721	3.728882478	3.909400152	4.971973012	5.228719954	6.019597217
6	1.674344512	2.821013285	3.728880067	3.909399042	4.971970945	5.228697680	6.019593962
$\alpha=\pi/12$(rad) $=15^\circ$, $x_{10}=3.73205081$							
q	κ_{11}	κ_{21}	κ_{01}	κ_{31}	κ_{41}	κ_{12}	κ_{51}
2	1.586196071	2.693060464	3.663679235	3.745778974	4.775069588	5.193122841	5.791041373
3	1.586186964	2.693019390	3.663437683	3.745692000	4.774930186	5.169025185	5.790847205
4	1.586185980	2.693014148	3.663406100	3.745679638	4.774908806	5.168412459	5.790815678
5	1.586185789	2.693013012	3.663399156	3.745676739	4.774903486	5.168319689	5.790807464
6	1.586185737	2.693012678	3.663397102	3.745675836	4.774901753	5.168297235	5.790804686
$\alpha=17\pi/180$(rad) $=17^\circ$, $x_{10}=3.27085262$							
q	κ_{11}	κ_{21}	κ_{01}	κ_{31}	κ_{41}	κ_{12}	κ_{51}
2	1.550087538	2.639709459	3.634259999	3.676853374	4.691504076	5.171679765	5.693465368
3	1.550079203	2.639670041	3.634023055	3.676768848	4.691368175	5.142562611	5.693276206
4	1.550078378	2.639665377	3.633993934	3.676757617	4.691348570	5.141963350	5.693247175
5	1.550078228	2.639664422	3.633987857	3.676755117	4.691343923	5.141875977	5.693239947
6	1.550078190	2.639664155	3.633986138	3.676754372	4.691342468	5.141855716	5.693237594
$\alpha=\pi/6$(rad) $=30^\circ$, $x_{10}=1.73205081$							
q	κ_{11}	κ_{21}	κ_{31}	κ_{01}	κ_{41}	κ_{12}	κ_{51}
2	1.304396116	2.263161756	3.180280275	3.385675476	4.080590720	4.976943610	4.971895069
3	1.304394835	2.263150480	3.180251425	3.385606099	4.080541084	4.922898138	4.971824214
4	1.304394775	2.263149774	3.180249222	3.385600542	4.080536711	4.922767198	4.971817250
5	1.304394769	2.263149685	3.180248908	3.385599799	4.080536025	4.922747436	4.971816072
6	1.304394767	2.263149668	3.180248843	3.385599654	4.080535873	4.922744256	4.971815795
$\alpha=\pi/4$(rad) $=45^\circ$, $x_{10}=1$							
q	κ_{11}	κ_{21}	κ_{31}	κ_{01}	κ_{41}	κ_{51}	κ_{12}
2	1.0	1.767377038	2.504928826	2.926575049	3.231122793	3.951541126	4.525856442
3	1.0	1.767376998	2.504928286	2.926574456	3.231121140	3.951537972	4.483062683
4	1.0	1.767376997	2.504928271	2.926574454	3.231121082	3.951537833	4.483018593
5	1.0	1.767376997	2.504928270	2.926574454	3.231121078	3.951537822	4.483018578
6	1.0	1.767376997	2.504928270	2.926574454	3.231121078	3.951537821	4.483018578

Table 1 (*continued*)

$\alpha=\pi/20$(rad) $=9^\circ$, $x_{10}=6.31375151$							
q	κ_{11}	κ_{21}	κ_{01}	κ_{31}	κ_{41}	κ_{12}	κ_{51}
$\alpha=\pi/3$(rad) $=60^\circ$, $x_{10}=0.577350269$							
q	κ_{11}	κ_{21}	κ_{31}	κ_{01}	κ_{41}	κ_{51}	κ_{12}
2	0.677682813	1.214432142	1.732050808	2.206458631	2.242653971	2.749809660	3.254991110
3	0.677679857	1.214431851	1.732050808	2.206457545	2.242653917	2.749809558	3.254990994
4	0.677679818	1.214431850	1.732050808	2.206457544	2.242653917	2.749809558	3.254990994
5	0.677679818	1.214431850	1.732050808	2.206457544	2.242653917	2.749809558	3.254990994
6	0.677679818	1.214431850	1.732050808	2.206457544	2.242653917	2.749809558	3.254990994

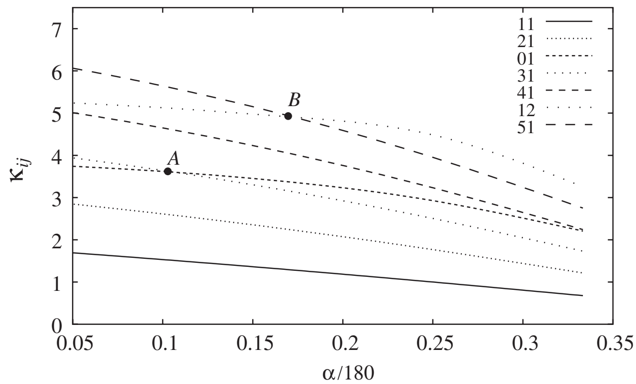

Fig. 5. Eigenvalues κ_{ij} versus α.

'split' of a multiple eigenvalue into simple eigenvalues may lead to secondary bifurcations of nonlinear sloshing regimes. In a forthcoming paper, we plan to conduct the corresponding nonlinear investigations.

3.2.5. Shapes of the natural surface modes

Fig. 6 shows surface modes defined by (24). Normalisation of these modes, which is usually accepted in nonlinear analysis (to interpret each generalised coordinate in (17a) as a generalised amplitude of F_{mn}), requires $\psi_{mn}(x_{10}, x_{20}) = 1$. It revises (27) to the form

$$\psi_{mn}(x_1, x_2) = \sum_{k=0}^{q} a_{nk}^{(m)} \left(\frac{x_1}{x_{10}}\right)^{v_{mk}} v_{v_{mk}}^{(m)}(x_2), \tag{35}$$

where

$$a_{nk}^{(m)} = \frac{\bar{a}_{nk}^{(m)}}{N_{mn}}; \quad N_{mn} = \psi_{mn}(x_{10}, x_{20}) = \sum_{k=0}^{q} \bar{a}_{nk}^{(m)} v_{v_{mk}}^{(m)}(x_{20}) \tag{36}$$

and $\{\bar{a}_{nk}^{(m)}\}$ are eigenvectors of (32).

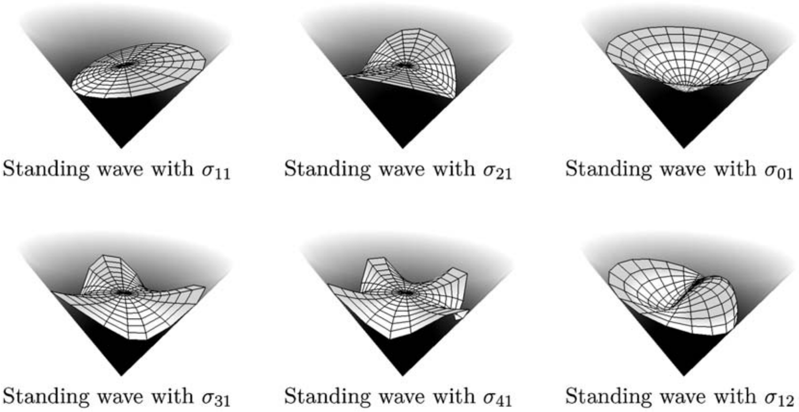

Fig. 6. Natural surface modes for $\pi/4(\mathrm{rad}) = 45^\circ$. The asymmetric modes (indexes 11, 21, 31, 41, 12) have double multiplicity, their shapes differ from each other by azimuthal rotation of 90°. (a) Standing wave with σ_{11}. (b) Standing wave with σ_{21}. (c) Standing wave with σ_{01}. (d) Standing wave with σ_{31}. (e) Standing wave with σ_{41}. (f) Standing wave with σ_{12}.

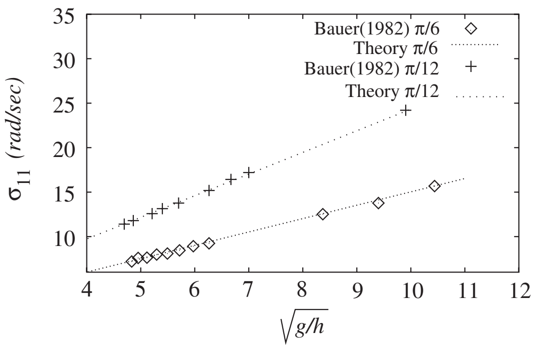

Fig. 7. The lowest natural frequency σ_{11} versus $\sqrt{g/h}$. Experimental measurements by Bauer (1982) are compared with our theoretical prediction.

3.3. Experimental validation

Bauer (1982) has performed experimental measurements of the lowest natural frequency σ_{11} for $\alpha = \pi/6(\mathrm{rad})$ (=30°) and $\alpha = \pi/12(\mathrm{rad})$ (=15°) and distinct fluid fillings (depths h). In order to compare our results with his experimental data, we note that $\sigma_{11} = \sqrt{\kappa_{11}x_{10}}\sqrt{g/h}$ and, therefore, $\sqrt{\kappa_{11}x_{10}}$, which is an invariant for a fixed α, determines a proportionality coefficient between σ_{11} and $\sqrt{g/h}$. Fig. 7 (σ_{11} versus $\sqrt{g/h}$) shows good agreement between our theoretical prediction and experimental results by Bauer (1982). A statistical experimental estimate of $\sqrt{\kappa_{11}x_{10}} = 1.63$ for $\alpha = 10^\circ$ was also published by Mikishev and Dorozhkin (1961). This value is consistent with our numerical prediction 1.67.

Numerical results in Fig. 5 show that the natural frequencies σ_{m1} are approximately in proportion to α (rad) and to $\sqrt{g/r_0}$, namely, $\sqrt{\kappa_{m1}x_{10}}/\alpha$ is a constant. This deduces the following formula $\sigma_{m1} = C_m\alpha\sqrt{g/r_0}$ (our calculations give, for instance, $C_1 = 0.6158$). Engineering of conical tanks may also be based on formula (23) and numerical results in Table 2.

Table 2
κ_{01}, κ_{11} and κ_{21} versus α

α°	κ_{01}	κ_{11}	κ_{21}
1	3.8228	1.8251	3.0323
3	3.8042	1.7925	2.9874
5	3.7844	1.7594	2.9414
7	3.7633	1.7258	2.8941
9	3.7407	1.6916	2.8457
11	3.7166	1.6570	2.7960
13	3.6909	1.6218	2.7451
15	3.6634	1.5862	2.6930
17	3.6340	1.5501	2.6397
19	3.6025	1.5135	2.5851
21	3.5689	1.4765	2.5293
23	3.5328	1.4390	2.4723
25	3.4943	1.4011	2.4140
27	3.4530	1.3627	2.3546
29	3.4088	1.3239	2.2939
31	3.3616	1.2848	2.2321
33	3.3110	1.2452	2.1691
35	3.2569	1.2052	2.1049
37	3.1991	1.1649	2.0396
39	3.1374	1.1242	1.9732
41	3.0715	1.0831	1.9056
43	3.0013	1.0417	1.8370
45	2.9266	1.0000	1.7674
47	2.8471	0.9580	1.6967
49	2.7628	0.9156	1.6250
51	2.6734	0.8730	1.5524
53	2.5789	0.8300	1.4788

4. Nonlinear sloshing in a conical tank

The nonlinear modal method, which is presented in this section, generalises results by Narimanov (1957), Lukovsky (1990) and Faltinsen et al. (2000, 2003). The method is based on the Moiseyev asymptotics and, therefore, it fails for shallow fluid flows characterised by progressive amplification of higher modes (Ockendon and Ockendon, 2001; Faltinsen and Timokha, 2002a).

4.1. Nonlinear modal system

We normalise the original free boundary problem (4) and its modal analogy (18) by r_0. This implies

$$\boldsymbol{g} := \frac{\boldsymbol{g}}{r_0}; \quad \dot{\boldsymbol{v}}_0 := \frac{\dot{\boldsymbol{v}}_0}{r_0}; \quad \beta_i(t) := \frac{\beta_i(t)}{r_0}; \quad R_i(t) := \frac{R_i(t)}{r_0^2}, \quad i \geqslant 1. \tag{37}$$

Furthermore, we consider the horizontal harmonic excitations

$$g_1=-g, \quad g_2=g_3=0; \quad v_{01}(t)=v_{02}(t)\equiv 0, \quad v_{03}=-\varepsilon\sigma \ \sin \ \sigma t, \tag{38}$$

where $\varepsilon \ll 1$ is the non-dimensional forcing amplitude and $\sigma \to \sigma_{11}$.

The Moiseyev asymptotics (Moiseyev, 1958; Gavrilyuk et al., 2000; Faltinsen et al., 2000) assumes that the lowest natural modes $F_{11}(x_2,x_3)=\psi_{11}(x_{10},x_2)^{\sin}_{\cos}x_3$ are of dominating character. By analysing this asymptotics for tanks of revolution, Lukovsky (1990) proposed and justified the five-dimensional approximate solutions

$$\begin{aligned} f^*(x_2,x_3,t) = x_{10} + f(x_2,x_3,t) &= x_{10} + \beta_0(t) + p_0(t) f_0(x_2) + [r_1(t)\sin x_3 \\ &\quad + p_1(t)\cos x_3] f_1(x_2) + [r_2(t)\sin 2x_3 + p_2(t)\cos 2x_3] f_2(x_2), \end{aligned} \tag{39}$$

$$\begin{aligned} \varphi(x_1,x_2,x_3) = {} & P_0(t)\psi_{01}(x_1,x_2) + [R_1(t)\sin x_3 + P_1(t)\cos x_3]\psi_{11}(x_1,x_2) \\ & + [R_2(t)\sin 2x_3 + P_2(t)\cos 2x_3]\psi_{21}(x_1,x_2), \end{aligned} \tag{40}$$

where $f_i(x_2)=\psi_{i1}(x_{10},x_2)$, $i=0,1,2$ (ψ_{i1} are normalised, see Section 3.2.5) and

$$r_1 \sim R_1 \sim p_1 \sim P_1 \sim \varepsilon^{1/3}; \quad p_0 \sim P_0 \sim r_2 \sim R_2 \sim p_2 \sim P_2 \sim \varepsilon^{2/3}. \tag{41}$$

When inserting (39) and (40) into the infinite-dimensional modal system (18) and accounting for (41), we get (correctly to $O(\varepsilon)$) the following nonlinear modal system coupling p_1, r_1, p_0, r_2 and p_2 (see its derivation in Appendix A):

$$\begin{aligned} & \ddot r_1 + \sigma_1^2 r_1 + \mathscr{D}_1(r_1^2\ddot r_1 + r_1\dot r_1^2 + r_1 p_1 \ddot p_1 + r_1 \dot p_1^2) \\ & \quad + \mathscr{D}_2(p_1^2 \ddot r_1 + 2p_1\dot r_1\dot p_1 - r_1 p_1 \ddot p_1 - 2r_1\dot p_1^2) - \mathscr{D}_3(p_2\ddot r_1 - r_2\ddot p_1 + \dot r_1\dot p_2 - \dot p_1\dot r_2) \\ & \quad + \mathscr{D}_4(r_1\ddot p_2 - p_1\ddot r_2) + \mathscr{D}_5(p_0\ddot r_1 + \dot r_1\dot p_0) + \mathscr{D}_6 r_1\ddot p_0 \\ & \quad + \sigma_1^2[\mathscr{G}_1 r_1(r_1^2+p_1^2) + \mathscr{G}_2(p_1 r_2 - r_1 p_2) + \mathscr{G}_3 r_1 p_0] + \Lambda \dot v_{03} = 0, \end{aligned} \tag{42a}$$

$$\begin{aligned} & \ddot p_1 + \sigma_1^2 p_1 + \mathscr{D}_1(p_1^2\ddot p_1 + p_1\dot p_1^2 + r_1 p_1 \ddot r_1 + p_1 \dot r_1^2) \\ & \quad + \mathscr{D}_2(r_1^2 \ddot p_1 + 2r_1\dot r_1\dot p_1 - r_1 p_1 \ddot r_1 - 2p_1\dot r_1^2) + \mathscr{D}_3(p_2\ddot p_1 + r_2\ddot r_1 + \dot r_1\dot r_2 + \dot p_1\dot p_2) \\ & \quad - \mathscr{D}_4(p_1\ddot p_2 + r_1\ddot r_2) + \mathscr{D}_5(p_0\ddot p_1 + \dot p_1\dot p_0) + \mathscr{D}_6 p_1\ddot p_0 \\ & \quad + \sigma_1^2[\mathscr{G}_1 p_1(r_1^2+p_1^2) + \mathscr{G}_2(r_1 r_2 + p_1 p_2) + \mathscr{G}_3 p_1 p_0] = 0, \end{aligned} \tag{42b}$$

$$\ddot r_2 + \sigma_2^2 r_2 - \mathscr{D}_9(p_1\ddot r_1 + r_1\ddot p_1) - 2\mathscr{D}_7\dot r_1\dot p_1 + \sigma_2^2[2\mathscr{G}_4 r_1 p_1] = 0, \tag{42c}$$

$$\ddot p_2 + \sigma_2^2 p_2 + \mathscr{D}_9(r_1\ddot r_1 - p_1\ddot p_1) + \mathscr{D}_7(\dot r_1^2 - \dot p_1^2) - \sigma_2^2[\mathscr{G}_4(r_1^2 - p_1^2)] = 0, \tag{42d}$$

$$\ddot p_0 + \sigma_0^2 p_0 + \mathscr{D}_{10}(r_1\ddot r_1 + p_1\ddot p_1) + \mathscr{D}_8(\dot r_1^2 + \dot p_1^2) + \sigma_0^2[\mathscr{G}_5(r_1^2 + p_1^2)] = 0. \tag{42e}$$

Here $\sigma_1=\sigma_{11}$, $\sigma_2=\sigma_{21}$ and $\sigma_0=\sigma_{01}$ are defined by (23) and Λ, $\mathscr{D}_i$ and $\mathscr{G}_i$, which depend only on α, are calculated by formulae (A.7). In order to help readers we give approximate values of these coefficients in Table 3. The modal system (42) differs from systems by Gavrilyuk et al. (2000) (circular cylindrical) and Faltinsen et al. (2003) (square-base) tanks by terms in the square brackets. These terms appear due to non-vertical walls, the coefficients $\mathscr{G}_i$ vanish as $\alpha \to 0$.

Since, to the authors' knowledge, the nonlinear fluid sloshing in a conical tank has never been studied and, as matter of fact, the modal system (42) has no analogies in the scientific literature, we tried our best to quantify its applicability. The quantification can be based on results by Ockendon et al. (1996), Ockendon

Table 3
Coefficients of the nonlinear modal system (42) versus α

α°	$\mathscr{D}_1$	$\mathscr{D}_2$	$\mathscr{D}_3$	$\mathscr{D}_4$	$\mathscr{D}_5$	$\mathscr{D}_6$	$\mathscr{D}_7$	$\mathscr{D}_8$	$\mathscr{D}_9$	$\mathscr{D}_{10}$
25	−0.1165	−0.4152	1.6116	−0.5428	2.0291	0.6715	0.6055	−0.3634	−1.2498	0.7113
27	−0.1927	−0.4287	1.6707	−0.5790	2.0773	0.7271	0.5954	−0.3428	−1.3445	0.8001
29	−0.2744	−0.4447	1.7330	−0.6163	2.1288	0.7833	0.5860	−0.3217	−1.4432	0.8964
31	−0.3623	−0.4635	1.7990	−0.6550	2.1838	0.8402	0.5773	−0.2999	−1.5465	1.0009
33	−0.4575	−0.4853	1.8691	−0.6953	2.2427	0.8980	0.5694	−0.2772	−1.6548	1.1146
35	−0.5609	−0.5106	1.9438	−0.7375	2.3060	0.9571	0.5623	−0.2536	−1.7689	1.2387
37	−0.6740	−0.5397	2.0236	−0.7818	2.3742	1.0177	0.5560	−0.2287	−1.8893	1.3742
39	−0.7984	−0.5731	2.1093	−0.8285	2.4478	1.0802	0.5506	−0.2026	−2.0170	1.5225
41	−0.9360	−0.6115	2.2015	−0.8780	2.5276	1.1450	0.5461	−0.1748	−2.1527	1.6851
43	−1.0891	−0.6556	2.3011	−0.9308	2.6145	1.2126	0.5426	−0.1454	−2.2978	1.8636
45	−1.2608	−0.7064	2.4092	−0.9872	2.7093	1.2837	0.5402	−0.1139	−2.4532	2.0600
47	−1.4546	−0.7650	2.5270	−1.0480	2.8134	1.3588	0.5390	−0.0802	−2.6207	2.2763
49	−1.6750	−0.8330	2.6559	−1.1136	2.9281	1.4389	0.5392	−0.0440	−2.8019	2.5153
51	−1.9277	−0.9123	2.7976	−1.1851	3.0552	1.5248	0.5408	−0.0050	−2.9990	2.7797
53	−2.2200	−1.0052	2.9543	−1.2633	3.1967	1.6179	0.5442	0.0372	−3.2146	3.073

α°	$\mathscr{G}_1$	$\mathscr{G}_2$	$\mathscr{G}_3$	$\mathscr{G}_4$	$\mathscr{G}_5$	Λ	k_1
25	−0.2541	0.6810	0.7638	0.4550	0.1446	1.3135	−0.1324
27	−0.2981	0.7388	0.8314	0.4965	0.1604	1.2872	−0.1425
29	−0.3469	0.7983	0.9007	0.5395	0.1774	1.2597	−0.1529
31	−0.4009	0.8597	0.9717	0.5841	0.1957	1.2311	−0.1634
33	−0.4607	0.9233	1.0448	0.6307	0.2155	1.2013	−0.1743
35	−0.5272	0.9896	1.1202	0.6795	0.2370	1.1704	−0.1855
37	−0.6012	1.0588	1.1984	0.7307	0.2603	1.1384	−0.1972
39	−0.6840	1.1316	1.2797	0.7848	0.2857	1.1054	−0.2094
41	−0.7768	1.2084	1.3647	0.8420	0.3136	1.0713	−0.2221
43	−0.8815	1.2899	1.4539	0.9028	0.3440	1.0361	−0.2356
45	−1.0000	1.3767	1.5482	0.9678	0.3774	1.0000	−0.2500
47	−1.1350	1.4697	1.6483	1.0376	0.4142	0.9629	−0.2653
49	−1.2897	1.5700	1.7552	1.1128	0.4548	0.9249	−0.2818
51	−1.4683	1.6787	1.8703	1.1944	0.4996	0.8859	−0.2997
53	−1.6760	1.7972	1.9951	1.2834	0.5493	0.8461	−0.3192

and Ockendon (2001) and Faltinsen and Timokha (2002a) that associate failure of the Moiseyev ordering (41) with the secondary (internal) resonance. The secondary resonance has also been discussed by Bryant (1989) (circular basin), it was examined for large amplitude forcing by Faltinsen and Timokha (2001) (rectangular tank) and La Rocca et al. (1997, 2000) and Faltinsen et al. (2003, 2005a) (square base tank). Quantification of critical semi-apex angles α, which yield the secondary resonance phenomena, can be done by analysing the dispersion relationship and higher periodic harmonics of steady-state solutions as $\sigma = \sigma_1$. Because of dramatical growth of the damping for higher harmonics and modes (Cocciano et al., 1991; Faltinsen and Timokha, 2002a; Faltinsen et al., 2005b), our analysis can be limited to the

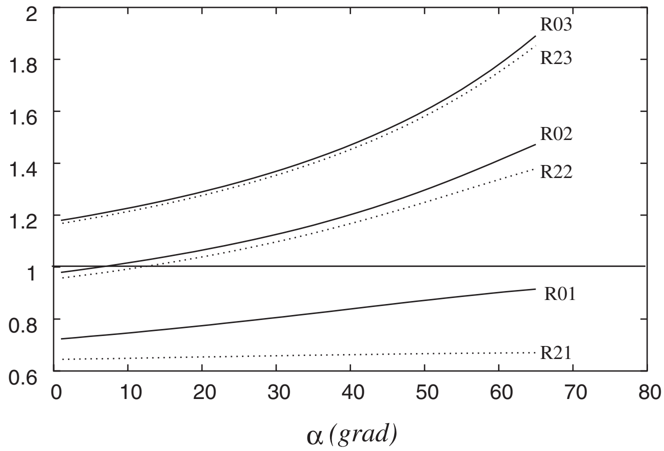

Fig. 8. $R0i$ and $R2i$ versus α.

second-order terms. In that case, influence of the secondary resonance is associated with the equalities

$$R0i = \frac{1}{2}\sqrt{\frac{\kappa_{0i}}{\kappa_{11}}} = 1, \quad R2i = \frac{1}{2}\sqrt{\frac{\kappa_{2i}}{\kappa_{11}}} = 1, \quad i \geqslant 1. \tag{43}$$

Fig. 8 shows the graphs of $R1i$ and $R0i$ versus α. Using the resonance conditions (43) we predict the secondary resonance about $\alpha = 6°$ (by mode 02) and $\alpha = 12°$ (by mode 22). When assuming $R0i$, $R2i$ close, but not equal to 1, for instance, $|R2i, R0i - 1| < 0.1$, we deduce that the Moiseyev-based modal system (42) is applicable for $25° < \alpha < 60°$.

4.2. Steady-state wave motions

By using (41) and accounting for results by Gavrilyuk et al. (2000) and Faltinsen et al. (2003), we pose the dominating modal functions of (39) as follows:

$$r_1(t) = A\cos\sigma t + \bar{A}\sin\sigma t + o(\varepsilon^{1/3}), \quad p_1(t) = \bar{B}\cos\sigma t + B\sin\sigma t + o(\varepsilon^{1/3}), \tag{44}$$

where A, $\bar{A}$, B and $\bar{B}$ are unknown constants (dominating amplitudes) and σ is the excitation frequency.

Representation (44) defines steady-state sloshing. By substituting (44) into (42c)–(42e) and gathering primary harmonics, the Fredholm alternative deduces

$$\begin{aligned} p_0(t) &= c_0 + c_1 \cos 2\sigma t + c_2 \sin 2\sigma t + o(\varepsilon^{2/3}), \\ p_2(t) &= s_0 + s_1 \cos 2\sigma t + s_2 \sin 2\sigma t + o(\varepsilon^{2/3}), \\ r_2(t) &= e_0 + e_1 \cos 2\sigma t + e_2 \sin 2\sigma t + o(\varepsilon^{2/3}), \end{aligned} \tag{45}$$

where

$$c_0 = l_0(A^2 + \bar{A}^2 + B^2 + \bar{B}^2); \quad c_1 = h_0(A^2 - \bar{A}^2 - B^2 + \bar{B}^2),$$
$$c_2 = 2h_0(A\bar{A} + B\bar{B}); \quad s_0 = l_2(A^2 + \bar{A}^2 - B^2 - \bar{B}^2),$$
$$s_1 = h_2(A^2 - \bar{A}^2 + B^2 - \bar{B}^2); \quad s_2 = 2h_2(A\bar{A} - B\bar{B}),$$
$$e_0 = -2l_2(A\bar{B} + B\bar{A}); \quad e_1 = 2h_2(\bar{A}B - A\bar{B}); \quad e_2 = -2h_2(AB + \bar{A}\bar{B}), \tag{46}$$

with

$$h_0 = \frac{\mathcal{D}_{10} + \mathcal{D}_8 - \bar{\sigma}_0^2\mathcal{G}_5}{2(\bar{\sigma}_0^2 - 4)}, \quad l_0 = \frac{\mathcal{D}_{10} - \mathcal{D}_8 - \bar{\sigma}_0^2\mathcal{G}_5}{2\bar{\sigma}_0^2},$$
$$h_2 = \frac{\mathcal{D}_9 + \mathcal{D}_7 + \bar{\sigma}_2^2\mathcal{G}_4}{2(\bar{\sigma}_2^2 - 4)}, \quad l_2 = \frac{\mathcal{D}_9 - \mathcal{D}_7 + \bar{\sigma}_2^2\mathcal{G}_4}{2\bar{\sigma}_2^2}; \quad \bar{\sigma}_m = \frac{\sigma_m}{\sigma}, \quad m = 0, 1, 2.$$

By inserting (44), (45) into (42a), (42b) and using the Fredholm alternative, we derive the following system of nonlinear algebraic equations coupling A, $\bar{A}$, B and $\bar{B}$:

$$A[\bar{\sigma}_1^2 - 1 - m_1(A^2 + \bar{A}^2 + \bar{B}^2) - m_2B^2] + m_3\bar{A}B\bar{B} = H\Lambda,$$
$$\bar{A}[\bar{\sigma}_1^2 - 1 - m_1(A^2 + \bar{A}^2 + B^2) - m_2\bar{B}^2] + m_3AB\bar{B} = 0,$$
$$B[\bar{\sigma}_1^2 - 1 - m_1(B^2 + \bar{A}^2 + \bar{B}^2) - m_2A^2] + m_3\bar{B}A\bar{A} = 0,$$
$$\bar{B}[\bar{\sigma}_1^2 - 1 - m_1(A^2 + B^2 + \bar{B}^2) - m_2\bar{A}^2] + m_3\bar{A}AB = 0, \tag{47}$$

where

$$m_1 = -\mathcal{D}_5\left(\tfrac{1}{2}h_0 - l_0\right) + \mathcal{D}_3\left(\tfrac{1}{2}h_2 - l_2\right) + 2\mathcal{D}_6h_0 + 2\mathcal{D}_4h_2 + \tfrac{1}{2}\mathcal{D}_1$$
$$- \bar{\sigma}_1^2\left[\tfrac{3}{4}\mathcal{G}_1 - \mathcal{G}_2\left(l_2 + \tfrac{1}{2}h_2\right) + \mathcal{G}_3\left(l_0 + \tfrac{1}{2}h_0\right)\right],$$
$$m_2 = \mathcal{D}_3\left(l_2 + \tfrac{3}{2}h_2\right) + \mathcal{D}_5\left(l_0 + \tfrac{1}{2}h_0\right) - 2\mathcal{D}_6h_0 + 6\mathcal{D}_4h_2 - \tfrac{1}{2}\mathcal{D}_1 + 2\mathcal{D}_2$$
$$- \bar{\sigma}_1^2\left[\tfrac{1}{4}\mathcal{G}_1 + \mathcal{G}_2(l_2 - \tfrac{3}{2}h_2) + \mathcal{G}_3(l_0 - \tfrac{1}{2}h_0)\right], \tag{48}$$
$$m_3 = m_2 - m_1.$$

System (47) is similar to Eqs. (14) by Gavrilyuk et al. (2000) (sloshing in circular cylindrical tanks); its resolvability condition is $m_3 \neq 0$. Solutions of (47) depend on the actual values of m_i which are functions of σ and α ($m_i = m_i(\sigma, \alpha)$). Taking into account that $\sigma \approx \sigma_1$, we can consider $m_i(\sigma_1, \alpha)$ (see the graphs in Fig. 9). These graphs establish that $m_3 > 0$ for $\alpha < 60°$ and $\sigma \to \sigma_1$.

Using derivations by Gavrilyuk et al. (2000) and Faltinsen et al. (2003) system (47) can be re-written to the equivalent form

$$A(\bar{\sigma}_1^2 - 1 - m_1A^2 - m_2B^2) = H\Lambda, \quad B(\bar{\sigma}_1^2 - 1 - m_1B^2 - m_2A^2) = 0, \quad \bar{A} = \bar{B} = 0. \tag{49}$$

Vanishing $\bar{A}$ and $\bar{B}$ makes it possible to treat A and B as dominating longitudinal (along oscillations of the tank) and transversal (perpendicular to the oscillations) amplitudes of steady-state waves, respectively. System (49) has only two classes of solutions. The first class suggests $B = 0$ and describes the so-called 'planar' regime. Eqs. (49) then take the following form:

$$A(\bar{\sigma}_1^2 - 1 - m_1A^2) = \Lambda H; \quad B = 0. \tag{50}$$

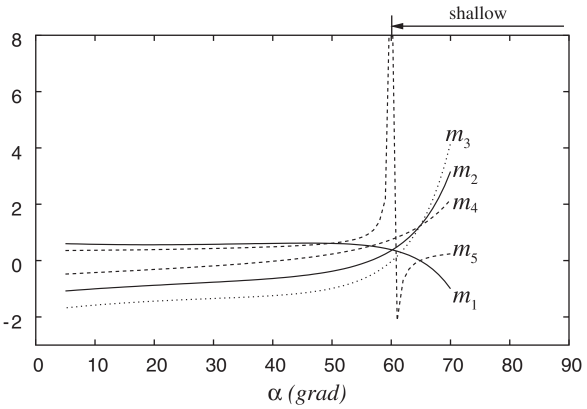

Fig. 9. $m_i(\sigma_1, \alpha)$ as functions of α.

The second class ($B^2 > 0$) describes the so-called 'swirling' regime (wave patterns imitate a rotation of the fluid volume around axis Ox). The algebraic system (49) then falls into the single equation with respect to A,

$$A(\bar{\sigma}_1^2 - 1 - m_4 A^2) = m_5 \Lambda H, \quad m_5 = -\frac{m_1}{m_3}, \quad m_4 = m_1 + m_2, \tag{51}$$

and the auxiliary formula for computing B

$$B^2 = \frac{1}{m_1}(\bar{\sigma}_1^2 - 1 - m_2 A^2) = \frac{1}{m_1}\left(m_5 \frac{\Lambda H}{A} + m_1 A^2\right) > 0. \tag{52}$$

Lukovsky (1990), Gavrilyuk et al. (2000) and Faltinsen et al. (2003) showed that response curves of 'planar' and 'swirling' depend on m_1 and m_4, respectively. Zeros of m_1 and m_4 at isolated semi-apex angles α imply a passage from the 'hard-spring' to 'soft-spring' behaviour. If $\alpha < 60°$, response curves of the 'planar' regime are always characterised by the 'soft-spring' behaviour (similar to the case of circular cylindrical tanks, Lukovsky, 1990). However, response curves of 'swirling' change their behaviour at $\alpha \approx 41.1°$ ($x_{10} = h/r_0 = 1.14\ldots$). Figs. 10 and 11 show the typical branching for $\alpha = 30°$ and $\alpha = 45°$, respectively. For the stability analysis the technique by Faltinsen et al. (2003) was used.

System (42) is linear in $\ddot{r}_i$, $\ddot{p}_i$. By inverting the matrix

$$\mathscr{A} = \begin{pmatrix} 1 + \mathscr{D}_1 r_1^2 + \mathscr{D}_2 p_1^2 - \mathscr{D}_3 p_2 + \mathscr{D}_5 p_0 & (\mathscr{D}_1 - \mathscr{D}_2) r_1 p_1 + \mathscr{D}_3 r_2 & -\mathscr{D}_4 p_1 & \mathscr{D}_4 r_1 & \mathscr{D}_6 r_1 \\ (\mathscr{D}_1 - \mathscr{D}_2) r_1 p_1 + \mathscr{D}_3 r_2 & 1 + \mathscr{D}_1 p_1^2 + \mathscr{D}_2 r_1^2 + \mathscr{D}_3 p_2 + \mathscr{D}_5 p_0 & -\mathscr{D}_4 r_1 & -\mathscr{D}_4 p_1 & \mathscr{D}_6 p_1 \\ -\mathscr{D}_9 p_1 & -\mathscr{D}_9 r_1 & 1 & 0 & 0 \\ \mathscr{D}_9 r_1 & -\mathscr{D}_9 p_1 & 0 & 1 & 0 \\ \mathscr{D}_{10} r_1 & \mathscr{D}_{10} p_1 & 0 & 0 & 1 \end{pmatrix}$$

it can be re-written to the normal form

$$\frac{d^2 \boldsymbol{p}}{dt^2} = \mathscr{A}^{-1} \boldsymbol{U}(t, \boldsymbol{p}, \dot{\boldsymbol{p}}), \tag{53}$$

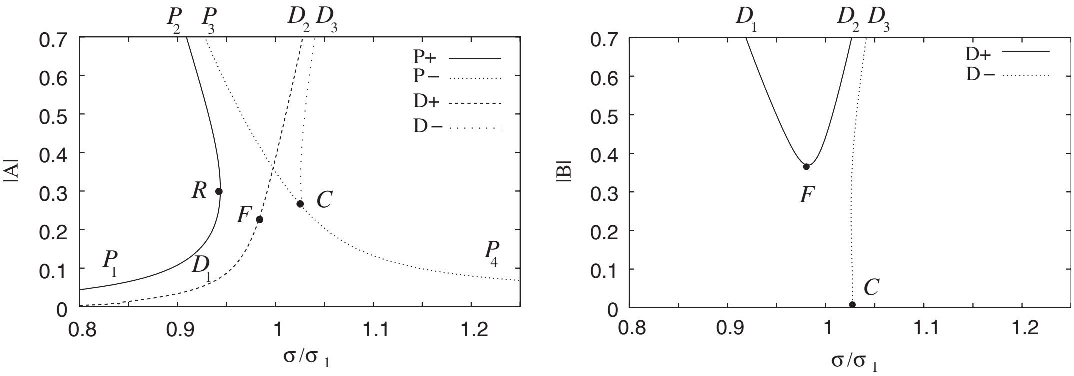

Fig. 10. Longitudinal (A) and transversal (B) amplitudes of steady-state resonant motions versus σ/σ_1. The results are given for $\alpha = 30^\circ$ and $H = 0.02$. Branches P_1P_2 and P_3P_4 imply 'planar', D_1D_2 denotes 'swirling' waves. R is the turning point, which divides the branch $P+$ into stable (P_1R) and unstable RP_2 subbranches. C is the Poincaré-bifurcation point. Here P_4C denotes the stable 'planar' solutions and CP_3 presents unstable ones. 'Swirling' is associated with the branches $D-$ and $D+$. The Hopf-bifurcation point F divides $D+$ into D_1F and FD_2, where D_1F implies unstable solutions, but FD_2 denotes a stable 'swirling'. There are no stable steady-state solutions for σ/σ_1 between abscissas of R and F.

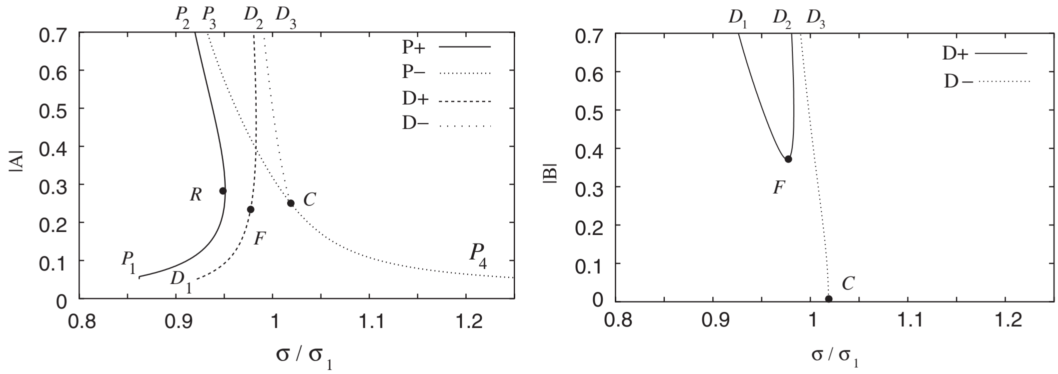

Fig. 11. The same as in Fig. 10, but for $\alpha = 45^\circ$.

where $\boldsymbol{p} = (r_1, p_1, r_2, p_2, p_0)^{\mathrm{T}}$ and

$$
\begin{aligned}
U_1 = & -\sigma_1^2(r_1 + \mathscr{G}_1 r_1(r_1^2 + p_1^2) + \mathscr{G}_2(p_1 r_2 - r_1 p_2) + \mathscr{G}_3 r_1 p_0) - \mathscr{D}_1 r_1(\dot{r}_1^2 + \dot{p}_1^2) \\
& - 2\mathscr{D}_2 \dot{p}_1(p_1 \dot{r}_1 - r_1 \dot{p}_1) + \mathscr{D}_3(\dot{r}_1 \dot{p}_2 - \dot{p}_1 \dot{r}_2) - \mathscr{D}_5 \dot{r}_1 \dot{p}_0 + \Lambda H \sigma^2 \cos \sigma t; \\
U_2 = & -\sigma_1^2(p_1 + \mathscr{G}_1 p_1(r_1^2 + p_1^2) + \mathscr{G}_2(r_1 r_2 + p_1 p_2) + \mathscr{G}_3 p_1 p_0) - \mathscr{D}_1 p_1(\dot{p}_1^2 + \dot{r}_1^2) \\
& - 2\mathscr{D}_2 \dot{r}_1(r_1 \dot{p}_1 - p_1 \dot{r}_1) - \mathscr{D}_3(\dot{r}_1 \dot{r}_2 + \dot{p}_1 \dot{p}_2) - \mathscr{D}_5 \dot{p}_1 \dot{p}_0; \\
U_3 = & -\sigma_2^2(r_2 + 2\mathscr{G}_4 r_1 p_1) + 2\mathscr{D}_7 \dot{r}_1 \dot{p}_1; \\
U_4 = & -\sigma_2^2(p_2 - \mathscr{G}_4(r_1^2 - p_1^2)) - \mathscr{D}_7(\dot{r}_1^2 - \dot{p}_1^2); \\
U_5 = & -\sigma_0^2(p_0 + \mathscr{G}_5(r_1^2 + p_1^2)) - \mathscr{D}_8(\dot{r}_1^2 + \dot{p}_1^2).
\end{aligned}
$$

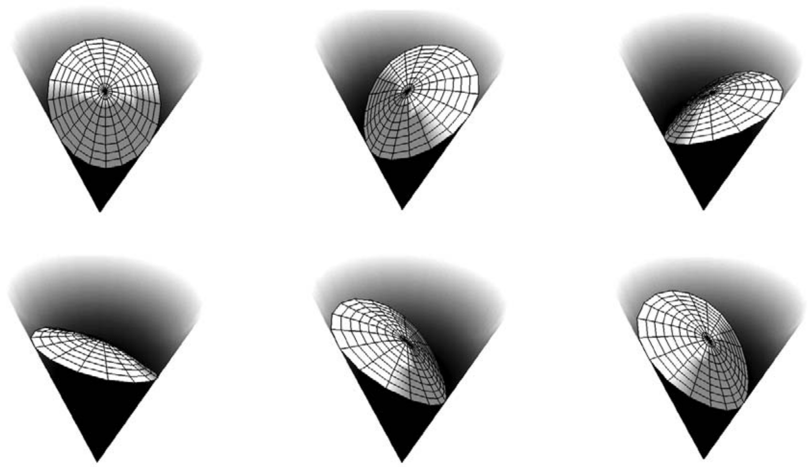

Fig. 12. Visualisation of 'swirling' for $\alpha = 30°$, $H = 0.02$, $\sigma/\sigma_1 = 0.9967$, $A = 0.35$, $B = 0.419$ with $r_1(0) = 0.35$, $p_2(0) = 0.122$, $p_0(0) = 0.469$, $\dot p_1(0) = 0.1494$, $\dot r_2(0) = 0.316$.

The initial conditions should define

$$\begin{aligned}&r_1(0) = r_1^0; \quad p_1(0) = p_1^0; \quad p_0(0) = p_0^0; \quad p_2(0) = p_2^0; \quad r_2(0) = r_2^0,\\ &\dot r_1(0) = \dot r_1^0; \quad \dot p_1(0) = \dot p_1^0; \quad \dot p_0(0) = \dot p_0^0; \quad \dot p_2(0) = \dot p_2^0; \quad \dot r_2(0) = \dot r_2^0.\end{aligned} \tag{54}$$

We solved the Cauchy problem (53), (54) by the fourth-order Runge–Kutta method. The simulations were made by a Pentium-II 366 computer. The simulation time depended on parameters of excitation. It varied between $\frac{1}{10}$ to $\frac{1}{300}$ of the real time-scale. Solutions (44), (45) made it possible to get initial conditions (54) to simulate steady-state regimes. These initial conditions were

$$\begin{aligned}&r_1(0) = A; \quad p_k(0) = A^2(l_k + h_k), \quad k = 0, 2; \quad p_1(0) = r_2(0) = 0,\\ &\dot r_k(0) = \dot p_k(0) = 0; \quad k = 1, 2; \quad \dot p_0 = 0\end{aligned} \tag{55}$$

for 'planar', and

$$\begin{aligned}&r_1(0) = A; \quad p_1(0) = 0; \quad p_2(0) = A^2(l_2 + h_2) + B^2(h_2 - l_2),\\ &p_0(0) = A^2(l_0 + h_0) + B^2(l_0 - h_0),\\ &\dot r_1(0) = 0; \quad \dot p_1(0) = \sigma B; \quad \dot r_2(0) = -4\sigma h_2 AB; \quad \dot p_2(0) = 0; \quad \dot p_0(0) = 0\end{aligned} \tag{56}$$

for 'swirling' regime, respectively.

Typical three-dimensional wave patterns are presented in Figs. 12–14. In particular, Figs. 13 and 14 illustrate the travelling wave phenomenon (see the movements of the crest *C*), which is explainable by contributions of the second-order modal functions r_2, p_2 and p_0.

5. Conclusions

Linear and nonlinear sloshing of an incompressible fluid in a conical tank was analysed within the framework of inviscid potential theory. Using a domain transformation technique by Lukovsky (1975)

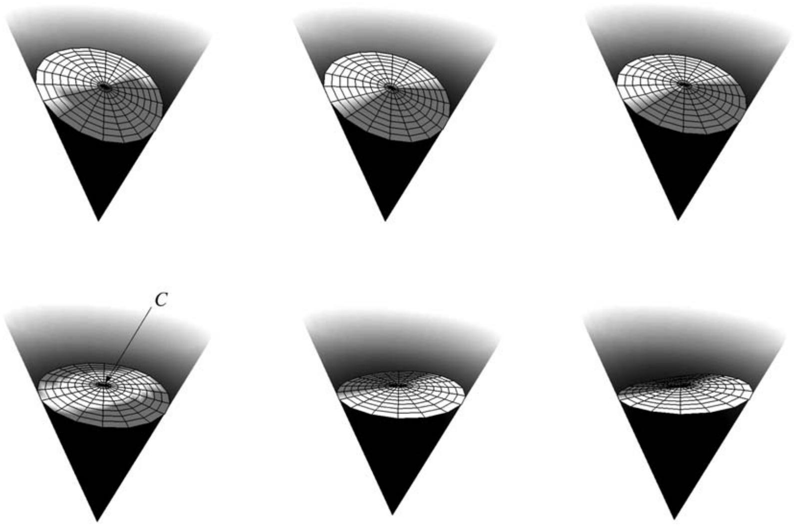

Fig. 13. Visualisation of 'planar' regime for $\alpha = 30°$, $H = 0.02$, $\sigma/\sigma_1 = 0.936$, $A = 0.2$ with $r_1(0) = 0.2$, $p_2(0) = -0.0117$, $p_0(0) = 0.00314$.

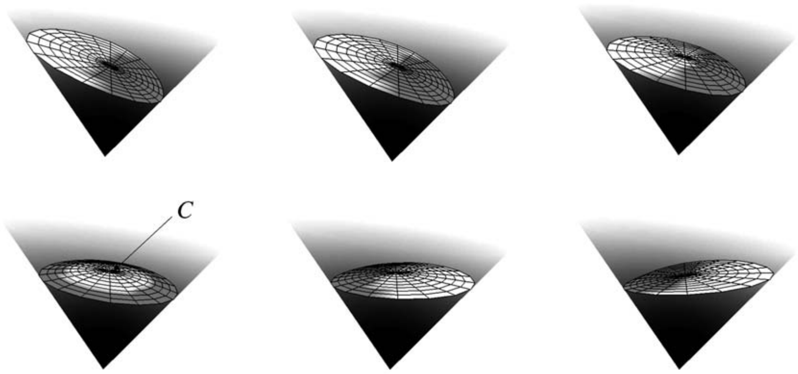

Fig. 14. Visualisation of 'planar' regime for $\alpha = 45°$, $H = 0.02$, $\sigma/\sigma_1 = 0.9463$, $A = 0.2$ with $r_1(0) = 0.2$, $p_2(0) = -0.011$, $p_0(0) = -0.1137$.

and a functional basis, which satisfies both the Laplace equation and the Neumann boundary condition on the tank walls, we found the approximate linear sloshing modes. The method guarantees 5–6 significant figures of the linear natural frequencies with only 5–6 basis functions. The numerical results were validated by experimental data.

By utilising the approximate linear natural modes and results by Lukovsky (1990) and Faltinsen et al. (2000), we derived a nonlinear finite-dimensional asymptotic modal system. The derived modal system is a novelty in the scientific literature. It couples five natural modes and makes it possible to analyse resonant sloshing due to a horizontal harmonic excitation with the forcing frequency close to the lowest natural frequency. Applicability of the modal system is limited by possible progressive activation of higher modes caused by secondary resonance. This was predicted for the semi-apex angles 6° and 12°. Besides, shallow fluid sloshing (Faltinsen and Timokha, 2002a; Ockendon and Ockendon, 2001) was quantified for $\alpha > 60°$. Our nonlinear modal theory should be applicable in the range $25° < \alpha < 60°$. Passage to $\alpha > 60°$ needs significant revisions of the present modal technique based on the Boussinesq asymptotics, in the manner of Faltinsen and Timokha (2002a).

The present paper is the first attempt to classify steady-state waves in conical tanks. The analysis finds 'planar' and 'swirling' steady-state regimes as well as a frequency domain, where 'chaotic' waves (there are no stable steady-state regimes) are realised. Advantages and possibilities of the modal system in engineering and for visualising realistic wave patterns were demonstrated. A further perspective can be a detailed study of 'chaotic' waves. The papers by Funakoshi and Inoue (1990, 1991) are useful in this context.

Appendix A. Derivation of the modal system

Solutions (39), (40) deal with $\{\tilde{F}_i(x_2, x_3)\}$, $\{\phi_n(x_1, x_2, x_3)\}$ and modal functions $\beta_i(t), R_i(t),\ i \geqslant 1$, of (17) as follows:

$$
\begin{aligned}
&\phi_1 = \psi_{01}; \quad \phi_2 = \psi_{11} \sin x_3; \quad \phi_3 = \psi_{11} \cos x_3; \quad \phi_4 = \psi_{21} \sin 2x_3; \quad \phi_5 = \psi_{21} \cos 2x_3,\\
&F_1 = f_0(x_2) = \psi_{01}(x_{10}, x_2); \quad F_2 = f_1(x_2) \sin x_3 = \psi_{11}(x_{10}, x_2) \sin x_3,\\
&F_3 = f_1(x_2) \cos x_3 = \psi_{11}(x_{10}, x_2) \cos x_3; \quad F_4 = f_2(x_2) \sin 2x_3 = \psi_{21}(x_{10}, x_2) \sin 2x_3,\\
&F_5 = f_2(x_2) \cos 2x_3 = \psi_{21}(x_{10}, x_2) \cos 2x_3,\\
&P_0(t) = Z_1(t); \quad R_1(t) = Z_2(t); \quad P_1(t) = Z_3(t); \quad R_2(t) = Z_4(t); \quad P_2(t) = Z_5(t),\\
&\beta_1(t) = p_0(t); \quad \beta_2(t) = r_1(t); \quad \beta_3(t) = p_1(t); \quad \beta_4(t) = r_2(t); \quad \beta_5(t) = p_2(t),
\end{aligned}
$$

where

$$
f_m(x_2) = a_{10}^{(m)} + \sum_{k=1}^{q} b_k^{(m)}(x_2); \quad b_k^{(m)}(x_2) = a_{1k}^{(m)} v_{vmk}^{(m)}(x_2), \quad m = 0, 1, 2.
$$

The time-dependent $\beta_0(t) = O(\varepsilon^{2/3})$ is a function of p_0, r_1, p_1, r_2 and p_2, i.e.

$$
\begin{aligned}
f^* = x_{10} + k_1(r_1^2(t) + p_1^2(t)) + p_0(t) f_0(x_2) + [r_1(t) \sin x_3\\
+ p_1(t) \cos x_3] f_1(x_2) + [r_2(t) \sin 2x_3 + p_2(t) \cos 2x_3] f_2(x_2),
\end{aligned} \tag{A.1}
$$

where the coefficient

$$
k_1 = -\frac{1}{x_{10}x_{20}^2} \int_0^{x_{20}} x_2 f_1^2(x_2)\, \mathrm{d}x_2
$$

is derived from the volume conservation condition

$$
|Q(t)| - |Q_0| = \int_0^{2\pi} \int_0^{x_{20}} \left(x_{10}^2 f + x_{10} f^2 + \frac{1}{3} f^3 \right) x_2\, \mathrm{d}x_2\, \mathrm{d}x_3 = 0
$$

considered correctly to $O(\varepsilon^{2/3})$.

The integrals A_n, A_{nk} and $\partial l_n/\partial\beta_i$ are linearly incorporated in (18) and, moreover, these integrals are linear in ρ. The density ρ can therefore be omitted. The integrals can be expanded in series by p_0, r_1, p_1, r_2 and p_2 correctly to $O(\varepsilon)$. Accounting for $\mathrm{d}A_n/\mathrm{d}t=\sum_{i=1}^{5}(\partial A_n/\partial\beta_i)\dot\beta_i$ and pursuing $O(\varepsilon)$ in $(\partial A_n/\partial\beta_i)\,\dot\beta_i$, $(\partial A_n/\partial\beta_i)\,Z_n$ and $A_{nk}Z_n$, $Z_n(\partial A_{nk}/\partial\beta_i)Z_k$ we get

$$\begin{aligned}
&A_1=a_4(r_1^2+p_1^2)+a_{17}p_0,\\
&A_2=a_5r_1+a_6r_1(r_1^2+p_1^2)+a_{18}(p_1r_2-r_1p_2)+a_{14}r_1p_0,\\
&A_3=a_5p_1+a_6p_1(p_1^2+r_1^2)+a_{18}(r_1r_2+p_1p_2)+a_{14}p_1p_0,\\
&A_4=a_{13}r_2-2a_7r_1p_1;\quad A_5=a_{13}p_2+a_7(r_1^2-p_1^2)
\end{aligned}\tag{A.2}$$

and

$$\begin{aligned}
&A_{11}=2a_1;\quad A_{21}=A_{12}=a_{15}r_1;\quad A_{31}=A_{13}=a_{15}p_1,\\
&A_{22}=2a_{10}+2a_{11}r_1^2+2a_{12}p_1^2+2a_9p_0-2a_{16}p_2,\\
&A_{32}=A_{23}=a_8r_1p_1+2a_{16}r_2;\quad A_{55}=A_{44}=2a_2,\\
&A_{33}=2a_{10}+2a_{11}p_1^2+2a_{12}r_1^2+2a_{16}p_2+2a_9p_0,\\
&A_{42}=A_{24}=a_3p_1;\quad A_{52}=A_{25}=-a_3r_1;\quad A_{43}=A_{34}=a_3r_1,\\
&A_{53}=A_{35}=a_3p_1;\quad A_{41}=A_{14}=A_{51}=A_{15}=A_{54}=A_{45}=0,
\end{aligned}\tag{A.3}$$

where coefficients $a_1,\dots,a_{18}$ are given by the following integrals:

$$a_1=\pi\int_0^{x_{20}}F_0^{(0,0)}(x_2)x_2\,\mathrm{d}x_2;\quad a_2=\frac{\pi}{2}\int_0^{x_{20}}(F_0^{(2,2)}(x_2)+\frac{4}{x_2^2}\,B_0^{(2,2)}(x_2))x_2\,\mathrm{d}x_2,$$

$$a_3=\frac{\pi}{2}\int_0^{x_{20}}(F_1^{(1,2)}(x_2)+\frac{2}{x_2^2}\,B_1^{(1,2)}(x_2))f_1(x_2)x_2\,\mathrm{d}x_2,$$

$$a_4=\pi\int_0^{x_{20}}(B_0^{(2)}(x_2)f_1^2(x_2)+2k_1B_0^{(1)}(x_2))x_2\,\mathrm{d}x_2,$$

$$a_5=\pi\int_0^{x_{20}}B_1^{(1)}(x_2)f_1(x_2)x_2\,\mathrm{d}x_2,$$

$$a_6=\pi\int_0^{x_{20}}\left(\tfrac{3}{4}\,B_1^{(3)}(x_2)f_1^2(x_2)+2k_1B_1^{(2)}(x_2)\right)f_1(x_2)x_2\,\mathrm{d}x_2,$$

$$a_7=-\frac{\pi}{2}\int_0^{x_{20}}B_2^{(2)}(x_2)f_1^2(x_2)x_2\,\mathrm{d}x_2,$$

$$a_8=\frac{\pi}{2}\int_0^{x_{20}}\left(F_2^{(1,1)}(x_2)-\frac{1}{x_2^2}\,B_2^{(1,1)}(x_2)\right)f_1^2(x_2)x_2\,\mathrm{d}x_2,$$

$$a_9=\frac{\pi}{2}\int_0^{x_{20}}\left[F_1^{(1,1)}(x_2)+\frac{1}{x_2^2}\,B_1^{(1,1)}(x_2)\right]f_0(x_2)x_2\,\mathrm{d}x_2,$$

$$a_{10}=\frac{\pi}{2}\int_0^{x_{20}}\left(F_0^{(1,1)}(x_2)+\frac{1}{x_2^2}\,B_0^{(1,1)}(x_2)\right)x_2\,\mathrm{d}x_2,$$

$$a_{11}=\frac{\pi}{2}\int_0^{x_{20}}\left(k_1\left[F_1^{(1,1)}(x_2)+\frac{1}{x_2^2}\,B_1^{(1,1)}(x_2)\right]\right.$$
$$\left.+\frac{3}{4}\left[F_2^{(1,1)}(x_2)+\frac{1}{3x_2^2}\,B_2^{(1,1)}(x_2)\right]f_1^2(x_2)\right)x_2\,\mathrm{d}x_2,$$

$$a_{12}=\frac{\pi}{2}\int_0^{x_{20}}\left(k_1\left[F_1^{(1,1)}(x_2)+\frac{1}{x_2^2}B_1^{(1,1)}(x_2)\right]\right.$$
$$\left.+\tfrac{3}{4}\left[\frac{1}{3}\,F_2^{(1,1)}(x_2)+\frac{1}{x_2^2}\,B_2^{(1,1)}(x_2)\right]f_1^2(x_2)\right)x_2\,\mathrm{d}x_2,$$

$$a_{13}=\pi\int_0^{x_{20}}B_2^{(1)}(x_2)f_2(x_2)x_2\,\mathrm{d}x_2,$$
$$a_{14}=2\pi\int_0^{x_{20}}B_1^{(2)}(x_2)f_0(x_2)f_1(x_2)x_2\,\mathrm{d}x_2;\quad a_{15}=\pi\int_0^{x_{20}}F_1^{(0,1)}(x_2)f_1(x_2)x_2\,\mathrm{d}x_2,$$
$$a_{16}=\frac{\pi}{4}\int_0^{x_{20}}\left[F_1^{(1,1)}(x_2)-\frac{1}{x_2^2}\,B_1^{(1,1)}(x_2)\right]f_2(x_2)x_2\,\mathrm{d}x_2,$$
$$a_{17}=2\pi\int_0^{x_{20}}B_0^{(1)}(x_2)f_0(x_2)x_2\,\mathrm{d}x_2;\quad a_{18}=\pi\int_0^{x_{20}}B_1^{(2)}f_1(x_2)f_2(x_2)x_2\,\mathrm{d}x_2.$$

Here, we introduce the functions $B_0^{(1)}$, $B_0^{(2)}$, $B_1^{(1)}$, $B_1^{(2)}$, $B_1^{(3)}$, $B_2^{(1)}$, $B_2^{(2)}$, $B_0^{(2,2)}$, $B_1^{(1,2)}$, $B_0^{(1,1)}$, $B_1^{(1,1)}$, $B_2^{(1,1)}$ and $F_0^{(0,0)}$, $F_0^{(1,1)}$, $F_0^{(2,2)}$, $F_1^{(0,1)}$, $F_1^{(1,2)}$, $F_1^{(1,1)}$, $F_2^{(1,1)}$ depending on $b_k^{(m)}(x_2)$ and

$$c_k^{(m)}(x_2)=a_{1k}^{(m)}\,\frac{\mathrm{d}v_{v_{mk}}^{(m)}}{\mathrm{d}x_2},\quad m=0,1,2;\quad k=0,1,\ldots,q.$$

These functions are expressed as follows:

$$B_m^{(1)}(x_2)=x_{10}^2\sum_{k=0}^{q}b_k^{(m)}(x_2);\quad B_m^{(2)}(x_2)=\frac{x_{10}}{2}\sum_{k=0}^{q}(v_{mk}+2)b_k^{(m)}(x_2),$$

$$B_m^{(3)}(x_2)=\frac{1}{6}\sum_{k=0}^{q}(v_{mk}+2)(v_{mk}+1)b_k^{(m)}(x_2),\quad m=0,1,2;$$

$$B_0^{(m,n)}(x_2)=x_{10}\sum_{i,j=1}^{q}\frac{b_i^{(m)}(x_2)b_j^{(n)}(x_2)}{v_{mi}+v_{nj}+1};\quad B_1^{(m,n)}=\sum_{i,j=1}^{q}b_i^{(m)}(x_2)b_j^{(n)}(x_2);$$

$$B_2^{(m,n)}=\frac{1}{2x_{10}}\sum_{i,j=1}^{q}(v_{mi}+v_{nj})b_i^{(m)}b_j^{(n)},\quad m,n=1,2;$$

$$\Pi_{ij}^{(m,n)}(x_2)=v_{mi}v_{nj}b_i^{(m)}b_j^{(n)}-x_2(v_{mi}b_i^{(m)}c_j^{(n)}+v_{ni}b_i^{(n)}c_j^{(m)})+(1+x_2^2)c_i^{(m)}c_j^{(n)},$$

$$F_0^{(m,n)}(x_2) = x_{10} \sum_{i,j=1}^{q} \frac{\Pi_{ij}^{(m,n)}(x_2)}{v_{mi} + v_{nj} + 1}; \quad F_1^{(m,n)}(x_2) = \sum_{i,j=1}^{q} \Pi_{ij}^{(m,n)}(x_2),$$

$$F_2^{(m,n)}(x_2) = \frac{1}{x_{10}} \sum_{i,j=1}^{q} (v_{mi} + v_{nj}) \Pi_{ij}^{(m,n)}(x_2), \quad m, n = 0, 1, 2.$$

Relationship (41) and $g_1 = -g$, $g_2 = g_3 = 0$ mean that the terms $\partial l_2/\partial\beta_i$ and $\partial l_3/\partial\beta_i$ of (18) should be calculated correctly to $O(1)$ as follows:

$$\frac{\partial l_2}{\partial\beta_i} = \begin{cases} 0, & \beta_i \not\equiv p_1, \\ \lambda, & \beta_i \equiv p_1, \end{cases} \quad \frac{\partial l_3}{\partial\beta_i} = \begin{cases} 0, & \beta_i \not\equiv r_1, \\ \lambda, & \beta_i \equiv r_1, \end{cases} \quad \lambda = x_{10}^3 \pi \int_0^{x_{20}} x_2^2 f_1(x_2)\, dx_2. \tag{A.4}$$

The scalar function l_1 reads as

$$\begin{aligned} l_1 = l_1^{(0)} &+ [l_1^{(1)}(r_1^2 + p_1^2) + l_1^{(2)} p_0^2 + l_1^{(3)}(r_2^2 + p_2^2) + l_1^{(4)}(r_1^2 + p_1^2)^2 \\ &+ l_1^{(5)}(\tfrac{1}{2} p_1^2 p_2 - \tfrac{1}{2} r_1^2 p_2 + r_1 p_1 r_2) + l_1^{(6)} p_0 (r_1^2 + p_1^2)], \end{aligned} \tag{A.5}$$

where

$$\begin{aligned} &l_1^{(0)} = \frac{\pi}{4} x_{10}^4 x_{20}^2; \quad l_1^{(1)} = \tfrac{1}{2} x_{10}^2 G_{11}; \quad l_1^{(2)} = \tfrac{1}{2} x_{10}^2 G_{00}; \quad l_1^{(3)} = \tfrac{1}{2} x_{10}^2 G_{22}, \\ &l_1^{(4)} = \tfrac{3}{16} G_{1111} + \tfrac{3}{2} x_{10} k_1 G_{11}; \quad l_1^{(5)} = 2 x_{10} G_{211}; \quad l_1^{(6)} = 2 x_{10} G_{011} \end{aligned}$$

and

$$\begin{aligned} &G_{00} = 2\pi \int_0^{x_{20}} x_2 f_0^2\, dx_2; \quad G_{11} = \pi \int_0^{x_{20}} x_2 f_1^2\, dx_2; \quad G_{22} = \pi \int_0^{x_{20}} x_2 f_2^2\, dx_2, \\ &G_{011} = \pi \int_0^{x_{20}} f_0 f_1^2 x_2\, dx_2; \quad G_{211} = \pi \int_0^{x_{20}} x_2 f_2 f_1^2\, dx_2; \quad G_{1111} = \pi \int_0^{x_{20}} x_2 f_1^4\, dx_2. \end{aligned}$$

Consider (18a) as a system of linear algebraic equations in $Z_k(t)$. Accounting for (A.2) and (A.3) and solving (18a) correctly to $O(\varepsilon)$ one obtains

$$\begin{aligned} R_1(t) = {} & Q_1 \dot r_1 + C_2 r_1^2 \dot r_1 + D_3 p_1^2 \dot r_1 + C_1 r_1 p_1 \dot p_1 \\ & + D_2(r_2 \dot p_1 - p_2 \dot r_1) + C_3(p_1 \dot r_2 - r_1 \dot p_2) + B_0 p_0 \dot r_1 + B_3 r_1 \dot p_0, \\ P_1(t) = {} & Q_1 \dot p_1 + C_2 p_1^2 \dot p_1 + D_3 r_1^2 \dot p_1 + C_1 p_1 r_1 \dot r_1 \\ & + D_2(r_2 \dot r_1 + p_2 \dot p_1) + C_3(r_1 \dot r_2 + p_1 \dot p_2) + B_0 p_0 \dot p_1 + B_3 p_1 \dot p_0, \\ P_0(t) = {} & C_0(r_1 \dot r_1 + p_1 \dot p_1) + D_0 \dot p_0; \quad R_2(t) = Q_2 \dot r_2 - D_1(r_1 \dot p_1 + p_1 \dot r_1), \\ P_2(t) = {} & Q_2 \dot p_2 + D_1(r_1 \dot r_1 - p_1 \dot p_1), \end{aligned} \tag{A.6}$$

where

$$C_0 = \frac{a_4}{a_1} - \frac{a_5 a_{15}}{4 a_1 a_{10}}; \quad D_0 = \frac{a_{17}}{2 a_1}; \quad C_1 = \frac{1}{a_{10}} \left(a_6 - \frac{a_4 a_{15}}{2 a_1} - \frac{a_5 a_8}{4 a_{10}} + \frac{a_5 a_{15}^2}{8 a_1 a_{10}} \right),$$

$$Q_2 = \frac{a_{13}}{2a_2};\quad C_3 = \frac{1}{2a_{10}}\left(a_{18} - \frac{a_3 a_{13}}{2a_2}\right);\quad B_0 = \frac{1}{2a_{10}}\left(a_{14} - \frac{a_5 a_9}{a_{10}}\right);\quad Q_1 = \frac{a_5}{2a_{10}},$$

$$B_3 = \frac{1}{2a_{10}}\left(a_{14} - \frac{a_{15}a_{17}}{2a_1}\right);\quad D_1 = \frac{a_7}{a_2} + \frac{a_3 a_5}{4a_2 a_{10}};\quad D_2 = \frac{1}{2a_{10}}\left(a_{18} - \frac{a_5 a_{16}}{a_{10}}\right),$$

$$D_3 = \frac{a_6}{2a_{10}} + Q_1\left(\frac{a_3^2}{4a_2 a_{10}} - \frac{a_{12}}{a_{10}} + \frac{a_3 a_7}{a_2 a_5}\right);\quad C_2 = D_3 + C_1.$$

Substituting (A.2)–(A.6) in (18b) and gathering the terms up to $O(\varepsilon)$ lead to the modal system (42a)–(42d), where

$$\mathscr{D}_1 = \frac{d_1}{\mu_1};\quad \mathscr{D}_2 = \frac{d_2}{\mu_1};\quad \mathscr{D}_3 = \frac{d_3}{\mu_1};\quad \mathscr{D}_4 = \frac{d_4}{\mu_1};\quad \mathscr{D}_5 = \frac{d_5}{\mu_1};\quad \mathscr{D}_6 = \frac{d_6}{\mu_1},$$

$$\mathscr{D}_7 = \frac{d_7}{\mu_2};\quad \mathscr{D}_8 = \frac{d_8}{\mu_0};\quad \mathscr{D}_9 = \frac{d_4}{\mu_2};\quad \mathscr{D}_{10} = \frac{d_6}{\mu_0};\quad \Lambda = \frac{\lambda}{\mu_1},$$

$$\mathscr{G}_1 = \frac{d_1^k}{\mu_1 \kappa_{11}};\quad \mathscr{G}_2 = \frac{2d_2^k}{\mu_1 \kappa_{11}};\quad \mathscr{G}_3 = \frac{2d_3^k}{\mu_1 \kappa_{11}};\quad \mathscr{G}_4 = \frac{d_2^k}{\mu_2 \kappa_{21}};\quad \mathscr{G}_5 = \frac{d_3^k}{\mu_0 \kappa_{01}}, \tag{A.7}$$

where

$$\mu_0 = a_{17} D_0;\quad \mu_1 = a_5 Q_1;\quad \mu_2 = a_{13} Q_2,$$
$$d_1 = 2a_4 C_0 + 2a_7 D_1 + a_5 C_2 + 3a_6 Q_1;\quad d_2 = a_5 D_3 + a_6 Q_1 + 2a_7 D_1,$$
$$d_3 = a_5 D_2 + a_{18} Q_1;\quad d_4 = 2a_7 Q_2 - a_5 C_3;\quad d_5 = a_5 B_0 + a_{14} Q_1,$$
$$d_6 = 2a_4 D_0 + a_5 B_3;\quad d_7 = d_4 + \tfrac{1}{2} d_3;\quad d_8 = d_6 - \tfrac{1}{2} d_5,$$
$$d_1^k = 4l_1^{(4)};\quad d_2^k = \tfrac{1}{2} l_1^{(5)};\quad d_3^k = l_1^{(6)}.$$

References

Abramson, H.N., 1966. The dynamics of liquids in moving containers. NASA Report, SP 106.

Bateman, H., Erdelyi, A., 1953. Higher Transcendental Functions. McGraw-Hill Book Company, Inc., New York, Toronto, London.

Bauer, H.F., 1982. Sloshing in conical tanks. Acta Mechanica 43 (3–4), 185–200.

Bauer, H.F., Eidel, W., 1988. Non-linear liquid motion in conical container. Acta Mech. 73 (1–4), 11–31.

Bauer, L., Keller, H.B., Reiss, E.L., 1975. Multiple eigenvalues lead to secondary bifurcation. SIAM Rev. 17, 101–122.

Bridges, T.J., 1987. Secondary bifurcation and change of type for three dimensional standing waves in finite depth. J. Fluid Mech. 179, 137–153.

Bryant, P.J., 1989. Nonlinear progressive waves in a circular basin. J. Fluid Mech. 205, 453–467.

Cariou, A., Casella, G., 1999. Liquid sloshing in ship tanks: a comparative study of numerical simulation. Mar. Struct. 12, 183–198.

Chester, W., 1968. Resonant oscillation of water waves. I. Theory. Proc. R. Soc. London 306, 5–22.

Chester, W., Bones, J.A., 1968. Resonant oscillation of water waves. II. Experiment. Proc. R. Soc. London 306, 23–30.

Cocciano, B., Faetti, S., Nobili, M., 1991. Capillary effects on surface gravity waves in a cylindrical container: wetting boundary conditions. J. Fluid Mech. 231, 325–343.

Dodge, F.T., Kana, D.D., Abramson, H.N., 1965. Liquid surface oscillations in longitudinally excited rigid cylindrical containers. AIAA J. 3 (4), 685–695.

Dokuchaev, L.V., 1964. On the solution of a boundary value problem on the sloshing of a liquid in conical cavities. App. Math. Mech. (PMM) 28, 151–154 (in Russian).

Eisenhart, L.P., 1934. Separable systems of stackel. Ann. Math. 35 (2), 284–305.

Faltinsen, O.M., 1974. A nonlinear theory of sloshing in rectangular tanks. J. Ship Res. 18, 224–241.

Faltinsen, O.M., Rognebakke, O.F., 2000. Sloshing. NAV 2000. Proceedings of the International Conference on Ship and Shipping Research, 19–22 September, 2000, Venice, Italy, pp. 56–68.

Faltinsen, O.M., Timokha, A.N., 2001. Adaptive multimodal approach to nonlinear sloshing in a rectangular rank. J. Fluid Mech. 432, 167–200.

Faltinsen, O.M., Timokha, A.N., 2002a. Asymptotic modal approximation of nonlinear resonant sloshing in a rectangular tank with small fluid depth. J. Fluid Mech. 470, 319–357.

Faltinsen, O.M., Timokha, A.N., 2002b. Analytically-oriented approaches to two-dimensional fluid sloshing in a rectangular tank (survey). Proceedings of the Institute of Mathematics of the Ukrainian National Academy of Sciences 44, pp. 321–345.

Faltinsen, O.M., Rognebakke, O.F., Lukovsky, I.A., Timokha, A.N., 2000. Multidimensional modal analysis of nonlinear sloshing in a rectangular tank with finite water depth. J. Fluid Mech. 407, 201–234.

Faltinsen, O.M., Rognebakke, O.F., Timokha, A.N., 2003. Resonant three-dimensional nonlinear sloshing in a square base basin. J. Fluid Mech. 487, 1–42.

Faltinsen, O.M., Rognebakke, O.F., Timokha, A.N., 2005a. Resonant three-dimensional nonlinear sloshing in a square base basin. Part 2. Effect of higher modes. J. Fluid Mech. 523, 199–218.

Faltinsen, O.M., Rognebakke, O.F., Timokha, A.N., 2005b. Classification of three-dimensional nonlinear sloshing in a square-base tank with finite depth. J. Fluids Struct. 20 (1), 81–103.

Feschenko, S.F., Lukovsky, I.A., Rabinovich, B.I., Dokuchaev, L.V., 1969. The Methods for Determining the Added Fluid Masses in Mobile Cavities. Naukova Dumka, Kiev (in Russian).

Frandsen, J.B., 2004. Sloshing motions in excited tanks. J. Comput. Phys. 196 (1), 53–87.

Funakoshi, M., Inoue, S., 1990. Bifurcations of limit cycles in surface waves due to resonant forcing. Fluid Dyn. Res. 5 (4), 255–271.

Funakoshi, M., Inoue, S., 1991. Bifurcations in resonantly forced water waves. Eur. J. Mech. B/Fluids 10 (2 Suppl.), 31–36.

Gavrilyuk, I., Lukovsky, I.A., Timokha, A.N., 2000. A multimodal approach to nonlinear sloshing in a circular cylindrical tank. Hybrid Methods Eng. 2 (4), 463–483.

Ibrahim, R.A., Pilipchuk, V.N., Ikeda, T., 2001. Recent advances in liquid sloshing dynamics. Appl. Mech. Res. 54 (2), 133–199.

La Rocca, M., Mele, P., Armenio, V., 1997. Variational approach to the problem of sloshing in a moving container. J. Theor. Appl. Fluid Mech. 1 (4), 280–310.

La Rocca, M., Sciortino, G., Boniforti, M.A., 2000. A fully nonlinear model for sloshing in a rotating container. Fluid Dyn. Res. 27, 23–52.

Landrini, M., Grytøyr, G., Faltinsen, O.M., 1999. A B-spline based BEM for unsteady free-surface flows. J. Ship Res. 13 (1), 13–24.

Landrini, M., Colagrossi, A., Faltinsen, O., 2003. Sloshing in 2-D flows by the SPH method. The 8th International Conference on Numerical Ship Hydromechanics, September 22–25, 2003, Busan, Korea.

Lukovsky, I.A., 1975. Nonlinear Oscillations of a Fluid in Tanks of Complex Shape. Naukova Dumka, Kiev. (in Russian).

Lukovsky, I.A., 1976. Variational method in the nonlinear problems of the dynamics of a limited liquid volume with free surface. In: Oscillations of Elastic Constructions with Liquid, Volna, Moscow, pp. 260–264 (in Russian).

Lukovsky, I.A., 1990. Introduction to the Nonlinear Dynamics of a Limited Liquid Volume. Naukova Dumka, Kiev. (in Russian).

Lukovsky, I.A., 2004. Variational methods of solving dynamic problems for fluid-containing bodies. Int. Appl. Mech. 40 (10), 1092–1128.

Lukovsky, I.A., Bilyk, A.N., 1985. Forced nonlinear oscillations of a liquid in a moving axial-symmetric conical tanks. In: Numerical-analytical Methods of Studying the Dynamics and Stability of Multidimensional Systems. Institute of Mathematics, Kiev, pp. 12–26 (in Russian).

Lukovsky, I.A., Timokha, A.N., 2002. Modal modeling of nonlinear fluid sloshing in tanks with non-vertical walls. Non-conformal mapping technique. Int. J. Fluid Mech. Res. 29 (2), 216–242.

Lukovsky, I.A., Barnyak, M.Ya., Komarenko, A.N., 1984. Approximate Methods of Solving the Problems of the Dynamics of a Limited Liquid Volume. Naukova Dumka, Kiev (in Russian).

Mikishev, G.N., Dorozhkin, N.Y., 1961. An experimental investigation of free oscillations of a liquid in containers. News of the Academy of Sciences of USSR, The Branch of Technical Sciences, Mechanics and Machinery (Izvestiya Akademii Nauk SSSR, Otdelenie Tekhnicheskikh Nauk Mekhanika: Mashinostroenie), vol. 4, pp. 48–53 (in Russian).

Miles, J.W., 1976. Nonlinear surface waves in closed basins. J. Fluid Mech. 75, 419–448.

Miles, J.W., 1984a. Internally resonant surface waves in a circular cylinder. J. Fluid Mech. 149, 1–14.

Miles, J.W., 1984b. Resonantly forced surface waves in a circular cylinder. J. Fluid Mech. 149, 15–31.

Minowa, C., 1994. Sloshing impact of rectangular water tank (water tank damage caused by Kobe Earthquake). Trans. Jpn. Soc. Mech. Eng., Part C 63 (612), 2643–2649.

Minowa, C., Ogawa, N., Harada, I., Ma David, C., 1994. Sloshing roof impact of rectangular tank. NASA Technical Report, DE94-012462.

Moan, T., Berge, S., 1997. Report of Committee I.2 "Loads". Proceedings of the 13th International Ship and Offshore Structures Congress, vol. 1. Pergamon, New York, pp. 59–122.

Moiseyev, N.N., 1958. To the theory of nonlinear oscillations of a limited liquid volume. Appl. Math. Mech. (PMM) 22, 612–621 (in Russian).

Narimanov, G.S., 1957. Movement of a tank partly filled by a fluid: the taking into account of non-smallness of amplitude. J. Appl. Math. Mech. (PMM) 21, 513–524 (in Russian).

Narimanov, G.S., Dokuchaev, L.V., Lukovsky, I.A., 1977. Nonlinear Dynamics of Flying Apparatus with Liquid. Mashinostroenie, Moscow. (in Russian).

NASA Space Vehicle Design Criteria (Structures), 1968. Propellant slosh loads. NASA SP-8009, August 1968.

NASA Space Vehicle Design Criteria (Structures), 1969. Slosh suppression. NASA SP-8031, May 1969.

Ockendon, J.R., Ockendon, H., 1973. Resonant surface waves. J. Fluid Mech. 59, 397–413.

Ockendon, H., Ockendon, J.R., 2001. Nonlinearity in fluid resonances. Meccanica 36, 297–321.

Ockendon, H., Ockendon, J.R., Waterhouse, D.D., 1996. Multi-mode resonance in fluids. J. Fluid Mech. 315, 317–344.

Parlett, B.N., 1998. The Symmetric Eigenvalue Problem. SIAM, Philadelphia, PA.

Rabinovich, B.I., 1975. Introduction to Dynamics of Spacecraft. Mashinostroenie, Moscow. (in Russian).

Shankar, P.N., Kidambi, R., 2002. A modal method for finite amplitude, nonlinear sloshing. Pramana—J. Phys. 59 (4), 631–651.

Solaas, F., 1995. Analytical and numerical studies of sloshing in tanks. Ph.D. Thesis, The Norwegian Institute of Technology, Trondheim.

Solaas, F., Faltinsen, O.M., 1997. Combined numerical and analytical solution for sloshing in two-dimensional tanks of general shape. J. Ship Res. 41, 118–129.